The Company of **Biologists**

RESEARCH ARTICLE

Malpighian tubules of caterpillars: blending RNAseq and physiology to reveal regional functional diversity and novel epithelial ion transport control mechanisms

Dennis Kolosov* and Michael J. O'Donnell

ABSTRACT

The Malpighian tubules (MTs) and hindgut constitute the functional kidney of insects. MTs are outpouchings of the gut and in most insects demonstrate proximodistal heterogeneity in function. In most insects, such heterogeneity is confined to ion/fluid secretion in the distal portion and ion/fluid reabsorption in the proximal portion. In contrast, MTs of larval Lepidoptera (caterpillars of butterflies and moths) are composed of five regions that differ in their association with the gut, their structure and ion/fluid transport function. Recent studies have shown that several regions can rapidly and reversibly switch between ion secretion and reabsorption. The present study employed RNAseq, pharmacology and electrophysiology to characterize four distinct regions of the MT in larval *Trichoplusia ni*. Luminal microelectrode measurements indicate changes in [K$^+$], [Na$^+$] and pH as fluid passes through different regions of the tubule. In addition, the regions examined differ in gene ontology enrichment, and demonstrate robust gradients in expression of ion transporters and endocrine ligand receptors. Lastly, the study provides evidence for direct involvement of voltage- and ligand-gated ion channels in epithelial ion transport of insect MTs.

KEY WORDS: Epithelial ion channels, Voltage-gated ion channels, Ligand-gated ion transporters, Mechanosensitive ion channels, Renal function model, Disease model

INTRODUCTION
Malpighian tubules of insects
In the vertebrate kidney, the primary filtrate is driven into the nephron using blood pressure within a closed circulatory system, juxtaposed to the kidney nephron (Kümmel, 1973; Schulte et al., 2015). In contrast, insects possess an open circulatory system and secretion of the primary urine is an osmotic consequence of active ion transport by their 'renal' tissues (Phillips, 1981). The Malpighian tubules (MTs) and hindgut together constitute the functional kidney of insects (Wigglesworth, 1961). The MTs secrete ions from the haemolymph into the tubule lumen, driving fluid secretion and enabling haemolymph clearance of toxins, xenobiotics and metabolites (O'Donnell, 2008). Water and ions in the primary urine are later reclaimed by the downstream segments of the MT and the hindgut (Phillips, 1981). As in the vertebrate nephron, MTs of insects are segmented into functionally distinct

Department of Biology, McMaster University, 524 Life Sciences Building, 1280 Main St West, Hamilton, Ontario, Canada L8S4K1.

*Author for correspondence (kolosovd@mcmaster.ca)

D.K., 0000-0003-3581-9991; M.J.O., 0000-0003-3988-6059

regions. At least two functionally distinct regions of the free MTs are present in most insect clades: the distal secretory segment (upstream) and the proximal reabsorptive segment (downstream, closer to the gut) (Phillips, 1981). However, MTs are quite diverse structurally and functionally: in different insect clades they vary in size, number, maximal fluid secretion rate and structural modifications (Phillips, 1981).

Cryptonephric condition of larval insects
The pinnacle of MT complexity is exemplified by the cryptonephric condition, developed by larvae of coleopterans (beetles), lepidopterans (caterpillars of butterflies and moths) and some hymenopterans (sawflies). In the cryptonephric condition, the blind distal end of the MT is closely applied to the gut and enveloped by a membrane to create a compartment, separate from the haemolymph-filled body cavity, forming the rectal complex (RC) (Fig. 1A).

Caterpillars are characteristically gluttonous, consuming three to four times their own body mass in food daily and increasing body size exponentially over several weeks (Gotthard, 2008). Larvae of many species are forest defoliators and pests of economically important crops (Dawkar et al., 2013). In order to make plant proteins more digestible, caterpillars secrete base equivalents into the midgut to establish a pH of ∼11, the highest measured in any biological system, to dissociate plant proteins from tannins (Berenbaum, 1980). Rapid growth, in turn, necessitates absorption of ions and water from the plant-based diet in order to expand haemolymph volume. It is thought that the main purpose of the cryptonephric condition in lepidopteran larvae is the recovery of water, ions and base equivalents from the gut, by way of the MTs, into the haemolymph (Kolosov and O'Donnell, 2019b). All of this is possible when the ion/water supply from the RC is plentiful, i.e. when the gut is full. However, this is not always the case.

When ion/water supply from the RC is not sufficient, for example, when the caterpillar ceases feeding just prior to a moult, parts of the free MT initiate ion and fluid secretion so as to allow clearance from the haemolymph of toxins and metabolites (Kolosov and O'Donnell, 2019b). In contrast to the mechanistic understanding of the RC of larval lepidopterans (see Audsley et al., 1993; Liao et al., 2000), our understanding of the mechanisms and regulation of ion transport in the distinct regions of the free MT is limited.

### Four distinct segments of the free MT
Emerging from the RC of lepidopteran larvae are six MTs, each consisting of a short rectal lead and four distinct major regions – the distal ileac plexus (DIP), the proximal ileac plexus (PIP), the yellow region (YR) and the white region (WR) (Fig. 1A). These regions differ in their association with the gut, gross morphology and transport of major electrolytes and fluid (Irvine, 1969; Ruiz-Sanchez et al., 2015; O'Donnell and Ruiz-Sanchez, 2015; Kolosov
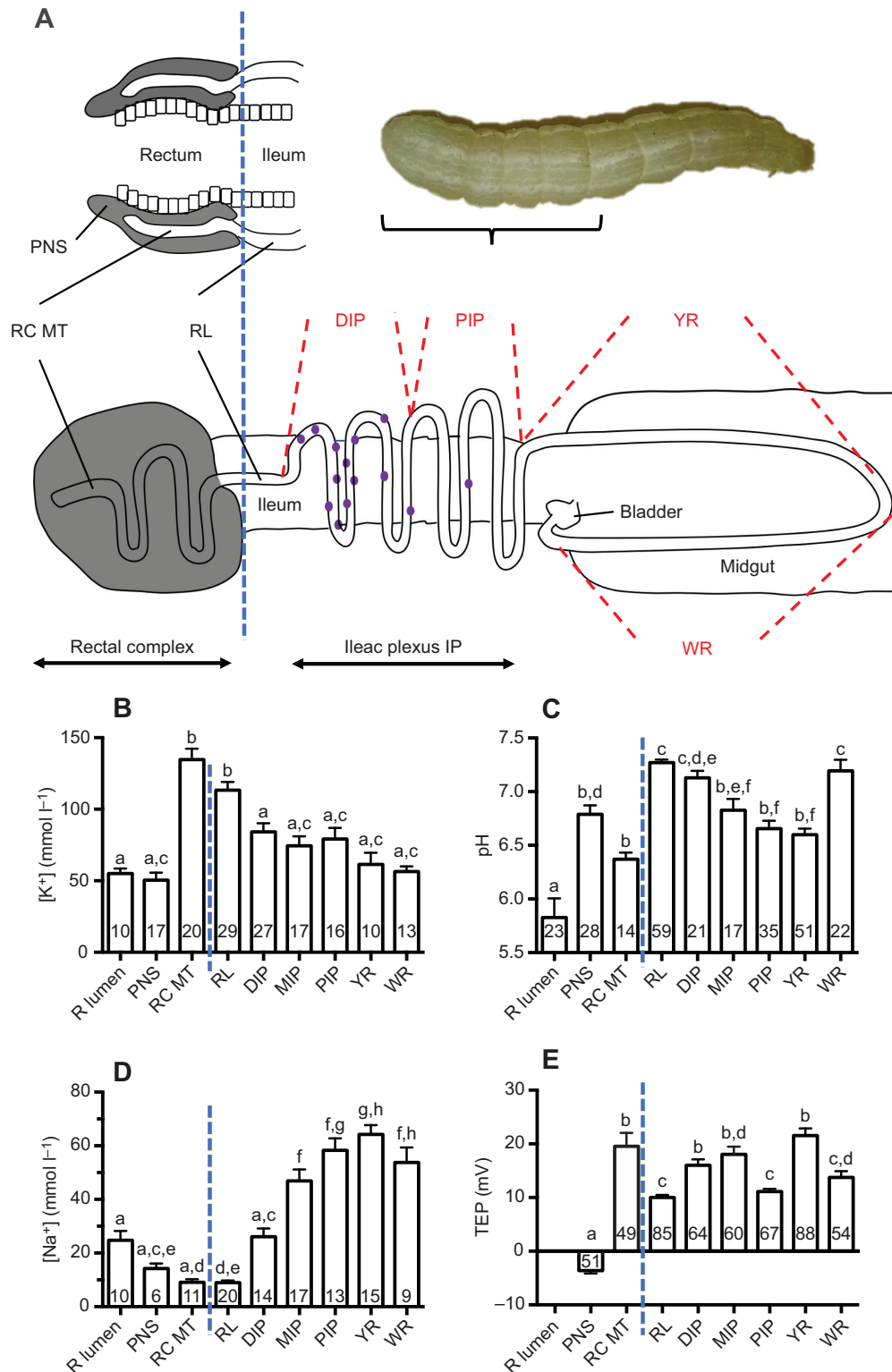
Fig. 1. Excretory system of the larval lepidopterans and modification of luminal ion content and transepithelial potential. (A) The blind distal end of each Malpighian tubule is embedded into the rectal complex (RC MT), suspended in the perinephric space (PNS), overlaid onto the underlying rectal epithelium and covered by the perinephric membrane (PM) – this constitutes the rectal complex. The rectal lead (RL) connects each RC MT to the downstream distal ileac plexus (DIP). The DIP contains most secondary cells (solid purple circles). Following the DIP, the proximal ileac plexus (PIP) terminates in the downstream yellow and white regions (YR and WR, respectively), which are closely applied to the posterior midgut, prior to terminating into the bladder at the midgut–hindgut juncture. Each of the compartments of the excretory system of larval *Trichoplusia ni* were impaled with self-referencing double-barrelled ion-selective microelectrodes to measure (B) $[K^+]$, (C) pH, (D) $[Na^+]$ and (E) transepithelial potential (TEP). All measurements were conducted on fed fifth instar larvae. Lowercase letters indicate significant differences as determined by a one-way ANOVA, followed by a Tukey's *post hoc* test. Number of replicates is indicated within each bar. R lumen, rectal lumen; MIP, middle ileac plexus.

and O'Donnell, submitted). Additionally, changes in luminal pH inferred from pH-sensitive dyes have been observed, suggesting that the free MT may play an important role in base recovery (Moffett, 1994).

The DIP is the most well-studied region to date – it is closely juxtaposed to the ileum and consists of the principal cells (PCs) and secondary cells (SCs) (O'Donnell and Ruiz-Sanchez, 2015). PCs and SCs are coupled by gap junctions (GJs) and transport K^+/Na^+ in opposite directions (Kolosov et al., 2018a). Unless the GJs are blocked, SCs always reabsorb K^+/Na^+ and secrete Cl^-, and this secretion is thought to play an important role in the reabsorption of HCO_3^- in the DIP (O'Donnell and Ruiz-Sanchez, 2015; Kolosov and O'Donnell, submitted). PCs, in contrast, secrete ions in larvae with empty guts, or when the DIP is transected experimentally so as to disconnect it from the RC, and switch to ion reabsorption in larvae fed ion-rich diets (Kolosov et al., 2018a,b, 2019a). This ability to change the direction of ion transport may be important for switching between the rectum (by way of the RC) and the haemolymph as a source of ions necessary to drive ion/fluid secretion in the MT. When PCs of the DIP switch to ion reabsorption, water and septate junction permeability are reduced to ensure that osmotically obliged water or harmful organics do not leak out of the tubule lumen back into the haemolymph (Kolosov and O'Donnell, 2019a,b; Kolosov et al., 2019b).

The PIP is directly downstream from the DIP. It consists mostly of PCs, and under normal dietary conditions reabsorbs K^+ and secretes Na^+ and Cl^- (O'Donnell and Ruiz-Sanchez, 2015). However, despite different ion-transporting properties of the DIP and PIP, many of the same ion transporters have been detected in both using conventional target-based approaches (Kolosov et al., 2018b).

The YR is directly downstream of the PIP and runs anteriorly along the posterior midgut, reabsorbing Na^+ and K^+, while secreting Cl^- (O'Donnell and Ruiz-Sanchez, 2015; Kolosov and O'Donnell, submitted). An early report suggests that YR is capable of secreting fluid when detached from the upstream ileac plexus (Irvine, 1969). Little is known about ion transport mechanisms and their regulatory networks in this region of the MT.

Lastly, the most downstream segment of the free MT is the WR – it runs posteriorly along posterior midgut. The WR has morphology distinctly different from the upstream regions: it appears thin-walled and often fills with uric acid crystals (Ryerse, 1979; O'Donnell and Ruiz-Sanchez, 2015). The WR reabsorbs K^+, Na^+ and Cl^- (O'Donnell and Ruiz-Sanchez, 2015; Kolosov and O'Donnell, submitted). Nothing is known about how this region works on a molecular basis, its functional specialization or the mechanisms involved in the regulation of its function.

Objectives and significance of the study
Although differences in the gross morphology of distinct free regions of the MT are apparent, the functional specialization of these regions, their mechanisms of ion and solute transport, as well as their regulation remain largely unknown. A recent RNAseq study profiled transcript expression in the DIP (Kolosov et al., 2019a), which can either secrete or reabsorb ions. However, in comparison with MTs of other insects, the majority of the length of lepidopteran MTs functions in ion reabsorption (Kolosov and O'Donnell, 2019b). Despite this, next to nothing is known about ion transport mechanisms and their regulation in reabsorptive segments of insect MTs.

The objective of the present study was to combine a variety of experimental approaches to characterize the functional diversity of the four distinct regions of the free MT in the larval *Trichoplusia ni* and describe putative region-specific regulatory mechanisms.

Although *Drosophila* MTs are accepted as an important model for human kidney development and function (Gautam et al., 2017; Millet-Boureima et al., 2018; Marelja and Simons, 2019; Davies et al., 2019), the MTs of lepidopteran larvae are more complex and regionalized, and by their close association with the gut, may better mimic distinct regions of the human nephron and their interaction with the interstitium of the kidney. They are larger and more easily accessible for electrophysiological study and measurements of ion fluxes across specific cell types. An emerging theme in studying larval lepidopteran MTs is that several regions of the tubule appear to respond to changes in the composition of the luminal fluids received from upstream regions (Irvine, 1969; Ruiz-Sanchez et al., 2015; Kolosov et al., 2018a,b). This may offer an opportunity for studying interactions between adjacent regions of the renal epithelium, similar to tubule–glomerular feedback of the vertebrate kidney. Therefore, understanding of how this happens mechanistically will allow for better understanding of insect renal function, and may aid development of animal models of kidney function and disease.

MATERIALS AND METHODS
Experimental animals
Eggs of the GLfc:IPQL:TniF04 strain (Roe et al., 2018) of *Trichoplusia ni* (Hübner 1800) were purchased from the Great Lakes Forestry Centre (Sault St Marie, ON, Canada). Larvae hatched in the laboratory and were maintained at 23–25°C with 40–50% relative humidity and fed a synthetic McMorran diet (McMorran, 1965). Feeding fifth instar larvae were used for all experiments in this study.

Measurement of transepithelial potential and luminal ion concentrations with double-barrelled ion-selective microelectrodes
Larvae were dissected under lepidopteran saline (O'Donnell and Ruiz-Sanchez, 2015; Maddrell and Gardiner, 1976) (in mmol l^{-1}) containing 15 NaCl, 30 KCl, 2 CaCl$_2$, 30 MgCl$_2$, 10 KHCO$_3$, 5 KHPO$_4$, 10 glucose, 10 maltose, 5 trisodium citrate, 10 glycine, 10 alanine, 10 proline, 10 glutamine, 10 valine, 5 serine and 5 histidine, pH 7.2. The body wall was removed so that the gut and adherent MTs remained intact, as described previously (O'Donnell and Ruiz-Sanchez, 2015). Regions of the free MT were separated from the gut and tracheae, pulled away from the gut and wrapped around poly-L-lysine-coated minutien pins secured in the layer of Sylgard on the bottom of a Petri dish. Transepithelial potential (TEP) and luminal ion concentration were measured simultaneously by impaling the tubule lumen with a microelectrode pulled from double-barrelled theta-glass (World Precision Instruments, Inc. Sarasota, FL, USA), where one barrel was filled with 150 mmol l^{-1} KCl at the tip (O'Donnell et al., 1998), and the second barrel was silanized with dichlorodimethylsilane (Sigma-Aldrich 440272), backfilled with an electrolyte solution and front-filled with an ionophore cocktail and backfill solution as follows: K^+: K^+ ionophore I, cocktail B (150 mmol l^{-1} KCl); Na^+: 3.5% Na^+ ionophore X, 95.9% o-nitrophenyl octyl ether, 0.6% potassium tetrakis chlorophenyl borate (150 mmol l^{-1} NaCl); and H^+: H^+ ionophore I, cocktail B (100 mmol l^{-1} NaCl, 100 mmol l^{-1} Na-citrate, pH 6). For TEP measurements alone, both barrels of the theta-glass microelectrode were filled with 150 mmol l^{-1} KCl. All potentials were measured with respect to a reference electrode consisting of an AgCl pellet connected to the bathing saline through a 3 mol l^{-1} KCl agar bridge. Potentials were recorded with a high impedance dual channel differential electrometer (HiZ-223; Warner Instruments,

Hamden, CT, USA) that was connected to a PowerLab data acquisition system running LabChart software (ADInstruments, Sydney, Australia).

Transmission electron microscopy

Procedures for TEM have been described in detail in Kolosov et al. (2019b). Briefly, distinct regions of the free MT were dissected out of a feeding fifth instar larvae and fixed in 2% glutaraldehyde and 4% paraformaldehyde in lepidopteran saline. Samples were then rinsed in saline, post-fixed in 1% osmium tetroxide in buffer, dehydrated in a graded ethanol series, followed by propylene oxide, and embedded in Quetol–Spurr resin. Thin sections were first heated to 80°C and then stained for 1 min in 1% Toluidine Blue. Sections were then rinsed with deionized water and air dried. Ultrathin 90 nm sections were cut on a Leica Ultracut microtome, stained with uranyl acetate and lead citrate and viewed in an FEI Tecnai 20 TEM (FEI, Hillsboro, OR, USA) at the NanoScale Bioimedical Imaging Facility (The Hospital for Sick Children Research Institute, Toronto, Canada).

RNA extraction and purification

RNA extraction for RNAseq experiments has been described in detail in Kolosov et al. (2019a). Briefly, free MT was dissected out of fifth feeding instar larvae in lepidopteran saline. Total RNA was extracted using Trizol reagent and following the manufacturer's instructions. Each region was separated from tracheae, excised from the MT and kept on ice immersed in RNAlater (Thermo Fisher Scientific). Six DIP, PIP, YR or WR samples originating from the same caterpillar were pooled together to constitute one biological replicate for molecular analysis. Three caterpillars were dissected. Samples were immersed in RNAlater and kept refrigerated as per the manufacturer's instructions. The following morning, RNAlater was removed by aspiration and tissues were immersed in 0.5 ml Trizol (Thermo Fisher Scientific) per six tubules. Tissues were homogenized in Trizol and total RNA extracted using isopropanol and 75% ethanol according to the manufacturer's instructions. Total RNA was purified using a Thermo Scientific GeneJet RNA Cleanup and Concentration Micro Kit (K#0841). The concentration and quality of purified RNA was determined using a NanoDrop spectrophotometer (ND-1000). Absorbance ratios of A_{260}/A_{280}=2.09±0.007 and A_{260}/A_{230}=2.25±0.05 were observed. Total RNA was sent to Génome Québec (McGill University, Montreal, Canada) for Illumina library preparation.

Illumina library preparation and next generation sequencing

Paired-end 100 bp Illumina libraries were prepared by Génome Québec using NovaSeq6000 S4 after subjecting total RNA samples to Bioanalyzer 2100 control screening. Libraries were generated from 250 ng of total RNA. mRNA enrichment was performed using the NEBNext Poly(A) Magnetic Isolation Module (New England BioLabs). cDNA synthesis was achieved with the NEBNext RNA First Strand Synthesis and NEBNext Ultra Directional RNA Second Strand Synthesis Modules (New England BioLabs). The remaining steps of library preparation were performed using the NEBNext Ultra II DNA Library Prep Kit for Illumina (New England BioLabs). Adapters and PCR primers were purchased from New England BioLabs, Next_dual sequences: AGATCGGAAGAGCAC-ACGTCTGAACTCCAGTCAC,AGATCGGAAGAGCGTCGTGT-AGGGAAAGAGTGT.

mRNA sequence read processing and quality control

Sequencing at McGill University and Génome Québec Innovation Centre (Montreal, QC, Canada) of 12 strand-specific libraries (3 DIP, 3 PIP, 3 YR and 3 WR) with 100-bp paired-end reads yielded 924,063,202 reads, with raw reads per library ranging from 66.6 million to 84.9 million reads, with a mean of 77 million. Quality control reports were performed by Génome Québec and 100% of reads with a read length of exactly 100 bp were subjected to quality control trimming with Trimmomatic (usegalaxy.org; Goecks et al., 2010). A total of 98% of reads remained paired after Trimmomatic quality control and were used in further analysis. In total, quality control resulted in the libraries yielding 908,600,000 reads, with raw reads per library ranging from 65.7 million to 83.7 million reads, with a mean of 75.7 million reads per library (all numbers associated with individual libraries can be found in Table S6).

Mapping to genomic transcriptome

The *T. ni* transcriptome was accessed at cabbagelooper.org and Official Gene Set v1.0 Transcripts were used for mapping (Fu et al., 2018). Mapping of next-generation sequencing reads to this transcript set was performed using Salmon (Galaxy version 0.9.1) mapping software on usegalaxy.org (Patro et al., 2017). Raw mapping results can be found in Table S5.

Differential expression analysis and interpretation

Differential expression (DE) analysis was performed in R (version 3.4.2) using the DESeq2 package (release 3.7) (Love et al., 2014), where all regions were independently compared with adjacent regions (DIP versus PIP, PIP versus YR and YR versus WR). This analysis resulted in three lists of all differentially expressed transcripts (Tables S1–S3) accompanied by the $\log_2$ fold-change ($\log_2$FC), *P*-value of the change and *P*-value adjusted (P_{adj}) for the false discovery rate (FDR) using the DESeq2 Benjamini–Hochberg algorithm. Only transcripts with $P_{adj}<0.05$ were considered differentially expressed and used in GO term enrichment analysis.

Regional gene ontology (GO) term enrichment

The GOSEQ package was used for GO term enrichment analysis (Young et al., 2010), a preferred method for RNAseq datasets as it avoids bias of highly expressed genes. GO term enrichment analysis was conducted using the goseq tool at usegalaxy.eu (version 1.34.0). Deseq2 results, transcript length and a many-to-many transcript-to-GO-term table (generated using the annotation released with the genomic transcriptome on cabbagelooper.org; Fu et al., 2018) were uploaded to Galaxy, where the Wallenius approximation of length bias correction and Benjamini–Hochberg false discovery rate ($P_{adj}<0.05$) corrections were used to calculate GO term enrichment. Enrichment in the DIP was assessed in relation to the downstream PIP. In the case of PIP, enrichment in relation to the upstream DIP, as well as the enrichment in relation to the downstream YR, were assessed separately. Likewise, enrichment in the YR was assessed in relation to the upstream PIP, as well as the downstream WR. Enrichment in the WR was assessed in relation to the upstream YR (see Table S4).

Normalized regional heterogeneity heatmaps

In order to visualize transcriptomic data in a functional manner, highlighting differences in regional expression of transcript, normalized regional heterogeneity heatmaps were constructed as follows. Transcripts per million (TPM) values indicative of transcript abundance were averaged for three samples stemming from the same region of the MT from different caterpillars (Table S5, TPM Summary tab). Average TPM values were then sorted and transcripts of interest identified (Table S5, Average values sorted tab). Transcripts were then broken into categories

(Table S5, ATPases, K^+ channels, Na^+ channels and exchangers, etc.). TPM values belonging to the same transporter were added for every region. Finally, a heatmap data list was compiled (Table S5, Heatmap data). In order to illustrate the differences in regional expression of the heatmap data transcripts, the data were normalized as follows. In every instance, all regional TPM values were divided by the maximal TPM value of the region with the highest expression of the transcript. This resulted in transcript expression values being represented in relation to the region with the highest expression, illustrating regional differences in expression of the same transcript rather than differences in expression between transcripts (see Table S5, Normalized heatmaps tab). Heatmaps were constructed using heatmap() function in R (version 3.4.2) (data are presented in Figs 4 and 6).

Scanning ion-selective electrode technique (SIET)

The hardware, software and methodology for acquiring SIET data and calculating ion fluxes have been described previously (Donini and O'Donnell, 2005; O'Donnell and Ruiz-Sanchez, 2015; Kolosov et al., 2018a). Briefly, SIET measurements were made with hardware from Applicable Electronics (Forestdale, MA, USA) and Automated Scanning Electrode Technique (ASET) software (version 2.0; Science Wares, Falmouth, MA, USA). Micropipettes were pulled on a P-97 Flaming-Brown pipette puller (Sutter Instruments Co., Novato, CA, USA) from 1.5-mm borosilicate glass (World Precision Instruments Inc., Sarasota, FL, USA). Microelectrodes were constructed with the following ionophores (Sigma-Aldrich, St Louis, MO, USA) (backfill and calibrating solutions in mmol l^{-1} indicated in brackets): Cl^- ionophore I, cocktail A (150 KCl backfill, 15/150 NaCl calibrations); K^+ ionophore I, cocktail B (150 KCl backfill, 15/150 KCl calibrations); and Na^+ ionophore X cocktail (3.5% Na^+ ionophore X, 95.9% o-nitrophenyl octyl ether, 0.6% potassium tetrakis chlorophenyl borate) (150 mmol l^{-1} NaCl).

The reference electrode used for SIET measurements consisted of a chloride Ag wire inserted into the back of a glass micropipette filled with 150 mm KCl. Alterations in bathing saline chloride concentration are known to change the liquid junction potential at the tip of such electrodes (Barry and Lynch, 1991; Neher, 1992). In order to minimize this change, the reference electrodes were constructed as follows: the length of pulled reference micropipette was increased by approximately one-third to allow for the tip and front one-third of the electrode to be filled with 150 mmol l^{-1} sodium acetate, while the back of the reference electrode was filled with 150 mmol l^{-1} KCl that was in contact with the AgCl-coated Ag wire. This arrangement eliminated diffusion of Cl^- from the tip of the reference electrode in contact with bathing solution but maintained Cl^- levels in contact with the silver wire, resulting in Nernstian slopes of ~63 mV per decade for the Cl^--selective microelectrode.

Measurements in different cell types of the DIP of *T. ni* were performed as previously described (O'Donnell and Ruiz-Sanchez, 2015; Kolosov et al., 2018a). At each measurement site, the ion-selective microelectrode voltage was measured close to the tissue (within 3–5 μm) and 50 μm further away from the tissue in three replicates. The mean measured voltage difference between the inner and outer limits of excursion was converted into a concentration difference using the following equation:

$$\Delta C = C_B \cdot 10^{(\Delta V/S)} - C_B, \qquad (1)$$

where ΔC is the concentration difference between the two points; C_B is the background ion concentration, calculated as the average of the concentrations at each point; ΔV is the difference in voltage between the inner and outer limits of excursion; and S is the slope of the electrode for a 10-fold change in concentration. Flux was estimated from the measured concentration difference using Fick's law:

$$J_I = D_I \Delta C / \Delta x, \qquad (2)$$

where J_I is the net flux of the ion in pmol cm^{-2} s^{-1}; D_I is the diffusion coefficient (Robinson and Stokes, 1968) of the ion (1.55×10^{-5} cm^2 s^{-1} for Na^+ and Cl^-, 1.92×10^{-5} cm^2 s^{-1} for K^+); ΔC is the concentration difference in μmol cm^{-3}; and Δx is the distance between the inner and outer limits of excursion measured in cm.

Effects of HCN blocker, GABA and glycine

Stock solution (100 mmol l^{-1} in DMSO) of ZD7288 (Sigma-Aldrich), an inhibitor of voltage-gated HCN channels, was diluted in saline to 10 μmol l^{-1} for SIET measurements; the final DMSO concentration in the bath did not exceed 0.01% v/v. Stimulation with 1 mmol l^{-1} GABA was achieved by replacing one-tenth of the volume of bathing saline with 10 mmol l^{-1} stock GABA solution in saline.

Glycine is a staple component of saline used in this study. Therefore, in order to be able to stimulate the MTs with glycine (Fig. 5), glycine-free saline was made, where glycine was replaced with mannitol. Stimulation of preparations with 1 mmol l^{-1} glycine for measurement of transepithelial or basolateral membrane potential was achieved by replacing one-tenth of the volume of glycine-free saline with '*Trichoplusia*' saline, which contains 10 mmol l^{-1} glycine.

ZD7288, GABA and glycine at concentrations used in this study did not affect the slopes or response time of ion-selective or double-barrelled TEP electrodes.

Immunohistochemistry procedures

Immunohistochemistry procedures have been described in detail in Kolosov et al. (2018a). Briefly, the DIP was dissected out from feeding fifth instar larvae, isolated and fixed in paraformaldehyde overnight at 4°C. The following day, tissues were dehydrated and rehydrated using a methanol:PBS gradient, blocked with antibody dilution buffer for 2 h at room temperature and incubated with primary antibodies overnight at 4°C. Primary antibodies for mouse anti-Cut and rat anti-Ttp were generously donated by Dr Barry Denholm (The University of Edinburgh) and Dr Laurent Fasano (Aix-Marseille Universite, CNRS, Marseille, France), respectively (Denholm et al., 2013). Following primary antibody incubation, tissues were washed in antibody dilution buffer and incubated with secondary chicken anti-rat Alexa Fluor 594 (catalogue no. A21471, Thermo Fisher Scientific) and FITC-conjugated goat anti-mouse (catalogue no. 115-095-146, Cedarlane, Burlington, Canada). Following incubation with secondary antibodies, tissues were mounted on the slides using DAPI-containing ProLong Antifade reagent (Thermo Fisher Scientific) and left to cure overnight. Slides were viewed the following day using a CTR-6500 laser-scanning confocal image acquisition system coupled to a Leica DM6000CS microscope at McMaster University imaging facilities.

Statistical analyses

Significant differences owing to experimental treatment were determined using a Student's *t*-test or a one-way ANOVA, followed by a Tukey's *post hoc* test as indicated in figure legends. All statistical tests were performed in GraphPad Prism 7 statistical software, which runs *t*-tests and ANOVAs alongside normality and equal variance tests. Significance was based on the observation of a *P*-value <0.05.

RESULTS

Ion content and pH of secreted fluid change in the lumen of MTs as the fluid passes through the tubule lumen

Luminal ion content of the fluid was monitored as it moved through adjacent compartments of the renal system of larval *T. ni*. Firstly, compared with the rectal lumen, $[Na^+]$ and $[K^+]$ in the perinephric space (PNS) were similar (Fig. 1B,D), whereas pH was significantly higher (Fig. 1C) and the TEP was inside-negative (Fig. 1E). Following this, in the RC MTs, $[K^+]$ increased dramatically, which coincided with the TEP becoming more positive (compared to the PNS), while $[Na^+]$ and pH did not change. As the fluid moved into the free tubule, in the rectal lead, its $[Na^+]$ and $[K^+]$ remained unaltered, but pH increased and TEP decreased. Finally, as the fluid moved through the regions of the free tubule, $[K^+]$ declined and $[Na^+]$ increased progressively, and pH decreased initially, increasing sharply only in the last WR segment. TEP was comparatively higher in the DIP and YR.

Substantial differences in ultrastructure and gene expression between adjacent regions of the MT

The DIP consists of two cell types, the PC and the SC, with substantial differences in their morphology (Fig. 2A). PCs exhibited prominent infoldings of apical membrane with apical crypts and microvilli that were filled with mitochondria (Fig. 2Ai). In contrast, the apical and basolateral membrane infoldings in the SCs are less extensive, with few mitochondria, evidence of vesicles budding off the apical membrane, and a short diffusional distance between the apical and basolateral membranes of ~2–3 μm (Fig. 2Aii). The PIP, in contrast, consisted largely of PCs (Fig. 2B) and exhibited extensive basolateral membrane infoldings and signs of vesicular traffic in the basolateral membrane (Fig. 2Bi).

The YR was characterized by massive apical infoldings, densely packed together (Fig. 2C,Ci). The basolateral membrane exhibited a subsurface layer filled with vesicular structures and associated particles resembling rough endoplasmic reticulum (Fig. 2Cii). This subsurface layer extended into the base of each apical crypt, following the infolding of the apical membrane. Epithelia of the WR appeared far more squamous (Fig. 3D), with lower cell height (Fig. 2Di), less convoluted apical membrane (Fig. 2Dii) and increased evidence of transepithelial vesicular traffic, with smaller vesicles originating in the basolateral membrane and larger vesicles present throughout the cell body and close to the apical membrane. Individual vesicles were often filled with concretions (Fig. 2Dii).
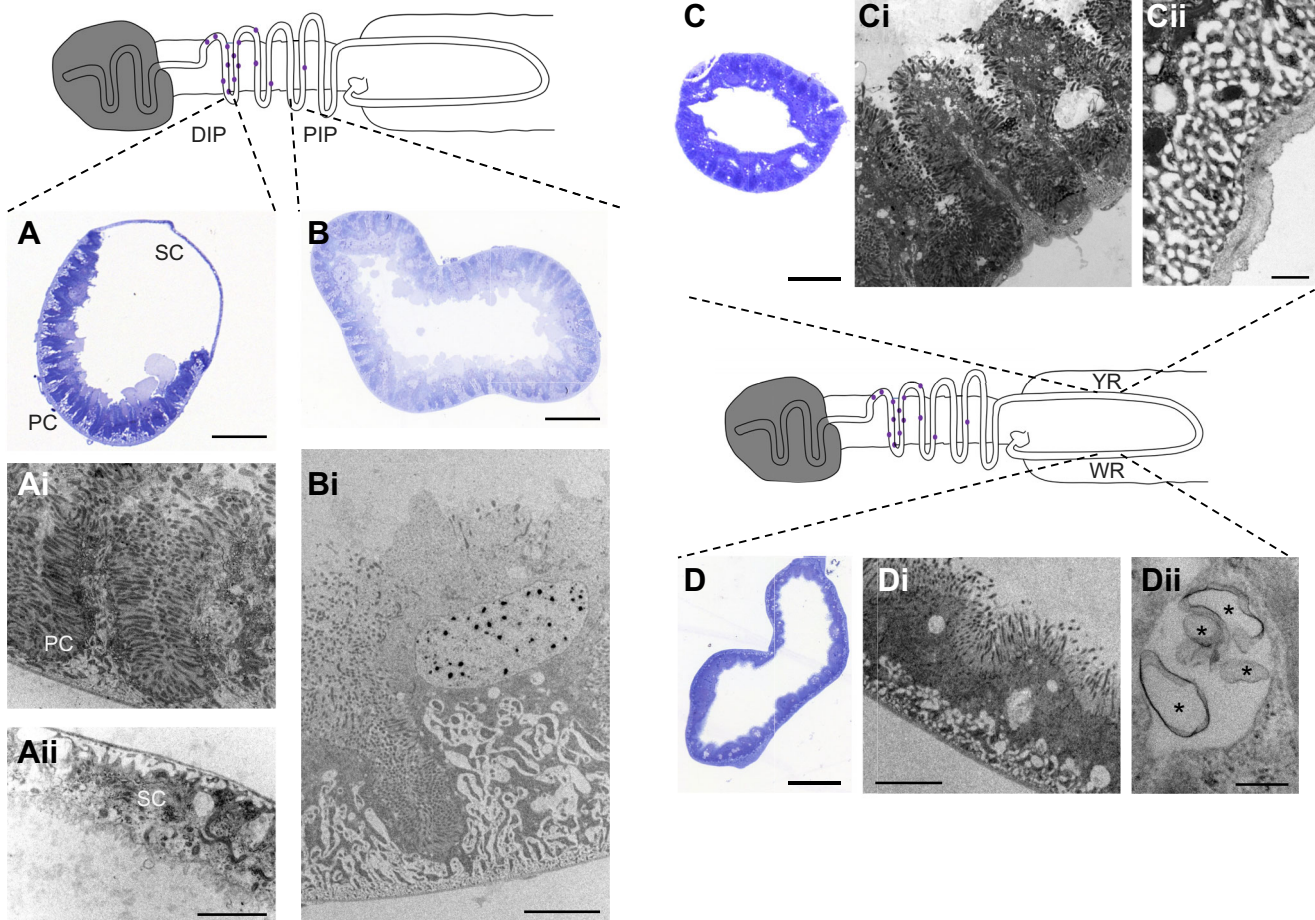

Fig. 2. Ultrastructural heterogeneity of the Malpighian tubule of larval *T. ni*. Representative transmission electron micrographs demonstrating regional ultrastructural differences between (A–Aii) the DIP, (B,Bi) the PIP, (C–Cii) the YR and (D–Dii) the WR. (A) Cross-section through the DIP containing both (A′) principal cells (PCs) and (Aii) secondary cells (SCs) highlights the difference in cell morphology between the two cell types. (A′) Extensive apical membrane infoldings in the DIP, (Bi) extensive basolateral membrane infoldings in the PIP, (C″) vesicular network lining basolateral membrane of the YR, which (Ci) extends into the apical infoldings, and (D′) transepithelial vesicular traffic in the WR with (Dii) vesicles containing concretions. Scale bars: 50 μm (A,B,C,D), 5 μm (Ai,Bi,Ci, Di), 2 μm (Aii), 500 nm (Dii) and 200 nm (Cii). Asterisks indicate concretions within vesicles in Dii.

Regional functional specialization evident from regional GO term enrichment

Principal component analysis revealed that all distinct regions clustered with like regions from different individual caterpillars (Fig. 3A). DE analysis demonstrated ample differences in transcript expression between adjacent regions of the tubule (Fig. 3B, Tables S1–S3). Comparisons of DIP and PIP transcriptomes revealed 1929 DE transcripts (950 expressed higher in the DIP
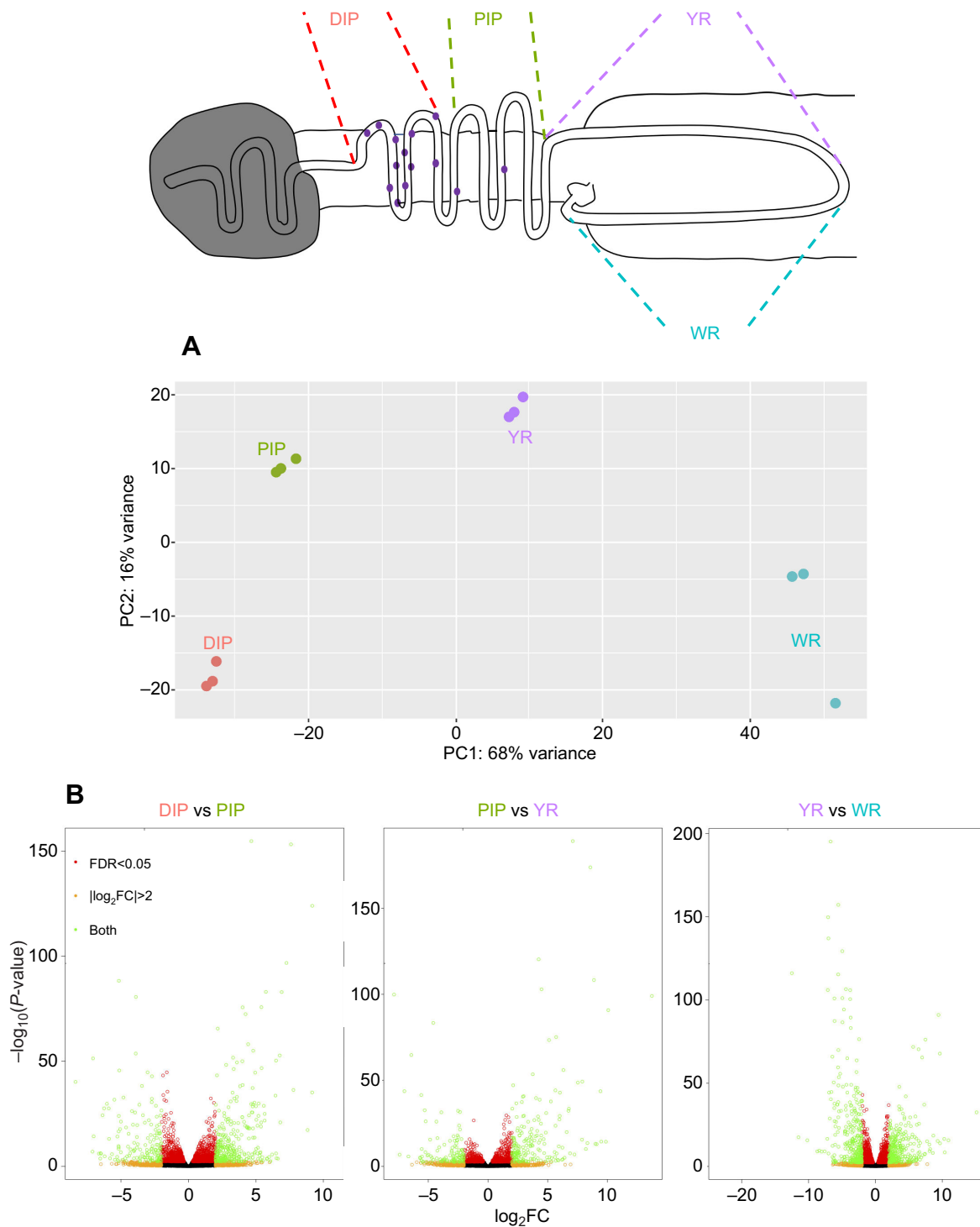
Fig. 3. Differential gene expression in four distinct regions of the Malpighian tubule of larval _T. ni_. (A) Principal component analysis conducted in R on four regions of the MT (three biological replicates each), which shows that the same regions from different biological replicates cluster with each other, and (B) differential expression analysis conducted with Deseq2 package in R using pairwise comparison of three biological replicates of adjacent regions of MT. Volcano plots show the fold-change in abundance of individual transcripts plotted against the $-\log_{10}(P\text{-value})$ of the change. Absolute values of $\log_2$ fold-change >2 ($|\log_2\text{FC}|>2$) are indicated in orange. Changes with FDR-adjusted $P_{\text{adj}}<0.05$ are indicated in red. Changes in both are indicated in green. Deseq2 results can be found in Tables S1–S3.

and 979 expressed higher in the PIP; Table S1); comparisons of PIP and YR transcriptomes revealed 977 DE transcripts (407 expressed higher in the PIP and 570 expressed higher in the YR; Table S2); and comparisons of YR and WR transcriptomes revealed 1995 DE transcripts (1091 expressed higher in the YR and 904 expressed higher in the WR; Table S3).

GO term enrichment analysis revealed that PIP, YR and WR were enriched in transcripts associated with xenobiotic transport and metabolism, as well as with carbohydrate metabolism (Table 1, Table S4). In addition, mitochondrial ATP metabolism, V-type H$^+$-ATPase transport, inward rectifier K$^+$ channels, and cAMP- and Ca^{2+}-based signalling transcripts were enriched in the DIP; the PIP was enriched in nitric oxide biosynthesis; the YR was enriched in amino acid transport and metabolism, polyamine biosynthesis and transcription processes; and the WR was enriched in ATPase activity coupled to transmembrane movement of substances.

Regional distribution of ion pumps, channels and transporters

Ion-motive ATPases, ion channels and co-transporters demonstrated regional heterogeneity in their expression. The DIP showed high levels of expression of V-type H$^+$- and plasma membrane Ca^{2+}-ATPases, as well as KCNK1, KCNK18, KCNT9, small conductance Ca^{2+}-activated (SK) K$^+$ channels, ClC2 Cl$^-$ channel and slc26a6 Cl$^-$/HCO$_3^-$ exchanger (CBE) (Fig. 4A). Additionally, the DIP expressed high levels of carbonic anhydrases (CA) 2, 3, 5, 10 and 13 and organic cation transporters (Fig. 4B). The PIP exhibited relatively higher levels of Kir2, Kir4, KCNK9 K$^+$ channels, as well as Mg^{2+} and Zn^{2+} transporters, but expressed KCNK18, slc26a6 and CA5 at levels similar to those in the DIP (Fig. 4A,B). The YR expressed relatively higher levels of KCNT7 K$^+$ channel, Ca^{2+} release-activated Ca^{2+} channel (CRaC), Na$^+$/H$^+$ exchanger (NHE) 10 and Multidrug Resistance Proteins (MRP), and levels of KCNK9 K$^+$ channel and Zn^{2+} transporters similar to the PIP. Lastly, WR exhibited relatively higher levels of Na$^+$/K$^+$-ATPase, Kir3, KCNK1, KCNT18, ORK1 and SK K$^+$ channels. Additionally, levels of Ryanodine Receptor (RyR) Ca^{2+} channel, Rh B ammonium channel, NHE8, SLC12A4 (KCC), slc12a9 (CCC6), slc4a1 (CBE), βCA, CA2 and slc41a1 Mg^{2+} transporters were higher than in the YR.

Na$^+$ channels and slc12a8 (cation–chloride cotransporter 9, CCC9) were more abundant in the DIP, PIP and YR compared with the WR. Aquaporins demonstrated the highest expression levels in the DIP with a decreasing trend toward the proximal regions of the MT. Ca^{2+}-gated Cl$^-$ channels (anoctamins), Na$^+$/H$^+$ exchanger 7 and Kir1 exhibited the same levels in all regions of the MT.

Expression of voltage-gated, ligand-gated and mechanosensitive ion channels

Several groups of voltage-gated (VGICs), ligand-gated (LGICs) and mechanosensitive ion channels were found to be expressed in all regions of the MTs (Fig. 4C). Notably, the DIP demonstrated higher expression of voltage-gated non-selective TRP, HCN and TPCN channels, as well as Ca$_V$1 and Ca$_V$3, and voltage-gated K$^+$ channels KCNC1, KCNQ1, KCNA3, KCNS1 and BK. Additionally, ligand-gated GABA/Na$^+$/Cl$^-$ co-transporter, Glu-gated Cl$^-$ channel and tetra-kcng channels were expressed highly in the DIP. In contrast, the PIP demonstrated higher expression of voltage-gated Ca$_V$2 and KCNH6. The YR was slightly enriched in cyclic nucleotide-gated (cng) channels. Lastly, voltage-gated KCNH1, KCNH8, KCNA3 and Na$^+$ channels, as well as the ligand-gated GlyR and mechanosensitive Piezo channels, demonstrated the highest expression in the WR.

Regulatory mechanisms: voltage-gated and ligand-gated ion channels

Because the DIP was found to be enriched in VGICs and LGICs, we utilized real-time ion flux measurements to determine whether stimulation or inhibition of these components had measurable effects on ion transport in the MTs of *T. ni*. Upon application of HCN inhibitor ZD7288 to isolated DIP preparations, PCs switched from K$^+$ secretion to K$^+$ reabsorption, while SCs remained unaffected (Fig. 5A). Similarly, application of GABA to the DIP resulted in reduced K$^+$ secretion, Na$^+$ reabsorption and increased Cl$^-$ secretion by the PCs, without affecting ion transport by the SCs (Fig. 5B). Because the WR demonstrated the highest expression of GlyR, the effects of glycine application were measured in this region. Using luminal and intracellular sharp electrode recordings, we demonstrated that application of glycine lead to changes in both transepithelial potential (TEP) and basolateral membrane potential (V$_{bl}$) (Fig. 5C).

Regulatory mechanisms: response to, and production of, endocrine ligands

Regional heterogeneity in the expression of endocrine receptors and several endocrine ligands was also evident in the free MT of the larval *T. ni*. In the DIP, levels of Allatostatin-A receptor were lower relative to the other three regions, and there was the highest expression of glutamate (metabotropic and ionotropic), acetylcholine, helicokinin, Neuromedin-U, neuropeptide F, as well as α1A adrenergic receptors (Fig. 6A). Additionally, the DIP expressed several neuropeptide ligands at relatively high levels: Bombyxin A2, short neuropeptide F, salivary secreted peptide and helicokinin precursor. Lastly, the DIP expressed vesicular transport proteins SV2a, SV2b and glutamate transporter. In contrast, the PIP demonstrated the highest levels of vesicular transport protein SV2c. The highest levels of 5-HT receptor, Neuromedin-B receptor and prostaglandin receptor, as well as Neuropeptide-like precursor, were detected in the YR. Lastly, the highest levels of metabotropic GABA, somatostatin, dopamine, ecdysone, tachykinin, diuretic hormone and LCGH receptors were detected in the WR compared with all other regions. The WR also exhibited the highest levels of diuretic hormone, allatostatin and orcokinin precursor ligands.

Cell–cell junctions

Levels of Inx-1 and -2 were highest in the DIP. In contrast, levels of Shaking-B and Inx-3 and -7 were highest in the WR (Fig. 6B). The WR showed the highest expression levels for all septate junction protein genes in the MTs of *T. ni*, with two notable exceptions: Tsp2A and Disks large were highest in the DIP.

Cell signalling, transcription factors and ligand processing

Relative expression levels of genes for ligand-processing enzymes, transcription factors and cell signalling mechanisms in each of the four tubule regions are shown in Fig. 6C. Ach-esterase, regucalcin, corticotrophin releasing factor (CRF)-binding protein orthologue, juvenile hormone (JH) esterase and JH-binding protein were all expressed at the highest levels in the WR. Prostaglandin reductase was detected at higher levels in the PIP and YR compared with the DIP and WR. The transcription factors Tiptop (Ttp) and Cut demonstrated reciprocal gradients in abundance along the length of the free tubule, with Ttp being most abundant in the DIP and Cut being most abundant in the WR. Similar to Cut, thyroid and CDX-2 transcription factors exhibited the highest levels of expression in the WR. Because Cut and Ttp have been implicated in PC–SC

Table 1. Gene ontology (GO) enrichment analysis (GOSEQ) in the distal ileac plexus, proximal ileac plexus, yellow and white regions of the free Malpighian tubule of the feeding fifth instar of larval *Trichoplusia ni*

GO term	GO term name	Notes
Distal ileac plexus		
Mitochondrial ATP metabolism		
GO:CC:0005739	Mitochondrion	Synthesis of ATP necessary to drive
GO:BP:0006119	Oxidative phosphorylation	active ion transport
GO:BP:0015986	ATP synthesis coupled proton transport	
GO:BP:0006120	Mitochondrial electron transport, NADH to ubiquinone	
GO:BP:0006099	Tricarboxylic acid cycle	
GO:CC:0045252	Oxoglutarate dehydrogenase complex	
GO:MF:0004591	Oxoglutarate dehydrogenase (succinyl-transferring) activity	
GO:CC:0045281	Succinate dehydrogenase complex	
GO:BP:0006123	Mitochondrial electron transport, cytochrome *c* to oxygen	
GO:MF:0004129	Cytochrome *c* oxidase activity	
GO:BP:0006555	Methionine metabolic process	
GO:MF:0030976	Thiamine pyrophosphate binding	
GO:CC:0000276	Mitochondrial proton-transporting ATP synthase complex, coupling factor F(o)	
GO:MF:0003954	NADH dehydrogenase activity	
VA-based H$^+$ transport		
GO:CC:0045261	Proton-transporting ATP synthase complex, catalytic core F(1)	Primary ion-motive drive for ion transport
GO:BP:0015991	ATP hydrolysis coupled proton transport	
GO:CC:0033179	Proton-transporting V-type ATPase, V0 domain	
GO:MF:0015078	Proton transmembrane transporter activity	
GO:MF:0046961	Proton-transporting ATPase activity, rotational mechanism	
GO:CC:0033180	Proton-transporting V-type ATPase, V1 domain	
Miscellaneous		
GO:MF:0005242	Inward rectifier potassium channel activity	Kir-based K$^+$ transport
GO:BP:0007224	Smoothened signalling pathway	GPCR pathway – increases cAMP levels
GO:MF:0005544	Calcium-dependent phospholipid binding	Calcium-dependent signalling
GO:CC:0032580	Golgi cisterna membrane	
GO:MF:0004013	Adenosylhomocysteinase activity	Amino acid biosynthetic pathway
Proximal ileac plexus		
Solute transport		
GO:BP:0055085	Transmembrane transport	Primary ion-motive drive for ion transport
GO:BP:0008152	Metabolic process	
GO:BP:0006811	Ion transport	
GO:CC:0016020	Membrane	
GO:MF:0042626	ATPase activity, coupled to transmembrane movement of substances	
Xenobiotic transport and metabolism		
GO:BP:0030001	Metal ion transport	
GO:MF:0046873	Metal ion transmembrane transporter activity	
GO:BP:0006749	Glutathione metabolic process	
GO:BP:0055114	Oxidation–reduction process	
GO:MF:0016491	Oxidoreductase activity	
GO:MF:0004416	Hydroxyacylglutathione hydrolase activity	
GO:MF:0016787	Hydrolase activity	
Nitric oxide biosynthesis		
GO:BP:0006809	Nitric oxide biosynthetic process	
GO:MF:0004517	Nitric oxide synthase activity	
Carbohydrate metabolism		
GO:BP:0006098	Pentose–phosphate shunt	
GO:BP:0006014	D-Ribose metabolic process	
GO:BP:0046835	Carbohydrate phosphorylation	
GO:MF:0016758	Transferase activity, transferring hexosyl groups	
Miscellaneous		
GO:MF:0004747	Ribokinase activity	Nucleotide biosynthesis
GO:MF:0010181	FMN binding	Binds to flavin mononucleotides
GO:MF:0004013	Adenosylhomocysteinase activity	Adenosine metabolism
GO:BP:0007020	Microtubule nucleation	*De novo* microtubule formation
GO:MF:0004815	Aspartate-tRNA ligase activity	Peptide biosynthesis/translation
GO:BP:0006555	Methionine metabolic process	?
Yellow region		
Solute transport		
GO:BP:0055085	Transmembrane transport	Amino acid transport and metabolism, polyamine biosynthesis
GO:BP:0003333	Amino acid transmembrane transport	Amino acid transport
GO:MF:0008483	Transaminase activity	Amino acid metabolism
GO:BP:0019467	Ornithine catabolic process, by decarboxylation	Polyamines can modulate ion channels
GO:MF:0008073	Ornithine decarboxylase inhibitor activity	

Table 1. Continued

GO term	GO term name	Notes
Transcription processes		
GO:BP:0032774	RNA biosynthetic process	Increased transcriptional activity?
GO:CC:0000428	DNA-directed RNA polymerase complex	
GO:MF:0008026	ATP-dependent helicase activity	
GO:BP:0009166	Nucleotide catabolic process	
Xenobiotic metabolism		
GO:BP:0055114	Oxidation-reduction process	
GO:MF:0016491	Oxidoreductase activity	
GO:MF:0008146	Sulfotransferase activity	
GO:MF:0016758	Transferase activity, transferring hexosyl groups	
GO:MF:0008191	Metalloendopeptidase inhibitor activity	
GO:MF:0005506	Iron ion binding	
Carbohydrate metabolism		
GO:BP:0006003	Fructose 2,6-bisphosphate metabolic process	
GO:BP:0005975	Carbohydrate metabolic process	
GO:MF:0004348	Glucosylceramidase activity	Degradation of polysaccharides
Miscellaneous		
GO:BP:0008152	Metabolic process	
GO:MF:0016787	Hydrolase activity	
GO:CC:0009343	Biotin carboxylase complex	Fatty acid biosynthesis
White region		
Solute transport		
GO:BP:0055085	Transmembrane transport	
GO:MF:0042626	ATPase activity, coupled to transmembrane movement of substances	Likely enrichment with NKA (see Fig. 4A)
Carbohydrate metabolism		
GO:BP:0006014	D-Ribose metabolic process	
Xenobiotic transport and metabolism		
GO:BP:0055114	Oxidation–reduction process	
GO:BP:0006749	Glutathione metabolic process	
GO:MF:0004416	Hydroxyacylglutathione hydrolase activity	
GO:MF:0046873	Metal ion transmembrane transporter activity	
GO:BP:0030001	Metal ion transport	
GO:MF:0016491	Oxidoreductase activity	
GO:MF:0004791	Thioredoxin–disulfide reductase activity	Defence against oxidative damage
Miscellaneous		
GO:MF:0004747	Ribokinase activity	Nucleotide biosynthesis
GO:CC:0016020	Membrane	
GO:BP:0008152	Metabolic process	

Raw GOSEQ results can be found in Table S4. CC, cell component; BP, biological process; MF, molecular function.

differentiation in insect MTs, we performed immunostaining to demonstrate that Cut localized exclusively to the PCs and Ttp localized exclusively to the SCs (Fig. 6C). Lastly, nitric oxide synthase (NOS) exhibited the highest levels of expression in the PIP.

DISCUSSION
Overview and significance
Much of the success of terrestrial insects is attributed to their ability to reabsorb virtually all the water and ions transported into the primary urine by the secretory segments of the MTs (Maddrell, 1981). This is especially important for lepidopteran larvae, which demonstrate one of the highest haemolymph volumes, as percentage of body mass, among insect clades, and in which haemolymph expansion and ion (K^+, HCO_3^-) reabsorption are crucial to their rapid growth (Maddrell, 1981).

Adjacent regions of insect MT have not been functionally characterized using next-generation sequencing tools prior to the present study. We have utilized a unique blend of electrophysiology, microscopy, next-generation sequencing and pharmacology to demonstrate that the regions are distinct in terms of: (i) functional specializations, (ii) novel molecular mechanisms of ion transport and putative regulatory control mechanisms, and (iii) discrimination between K^+-secretory and K^+-reabsorptive machinery. We have directly demonstrated that

the DIP, PIP, YR and WR differ in ultrastructure, gene expression and function, modifying fluid secreted by the RC as it passes through them, much like the nephron of the human kidney does. Notably, this study directly implicates voltage- and ligand-gated ion channels and transporters in the regulation of ion transport in the MTs. Lastly, this study indicates that insect renal tissues may participate in the autocrine and paracrine regulation of their function, possibly contributing to the production and clearance of endocrine ligands.

The rectal complex actively absorbs ions and base from the gut
In the present study, it appears that K^+ and HCO_3^- are actively transported into the RC, while Na^+ may be transported passively. Firstly, increased pH and inside-negative TEP in the PNS (Fig. 1C) are indicative of base reabsorption and the presence of a Cl^- pump in the rectal epithelium, consistent with previous reports (Moffett, 1994; Onken and Moffett, 2017; Kolosov and O'Donnell, 2019b; Liao et al., 2000). Cations, in turn, may follow by diffusion across the rectal epithelium because their concentrations in the rectal lumen and PNS are not different (Fig. 1B,D). Ion transport in the RC is likely aided by a combination of the previously reported NKCC, KCC, NBC-3 and Kir1 (Audsley et al., 1993; Kolosov et al., 2018a). Cation concentrations in the RC MT lumen are similar to (Na^+) or above (K^+) those in the PNS, and because the TEP of the RC MT is inside-
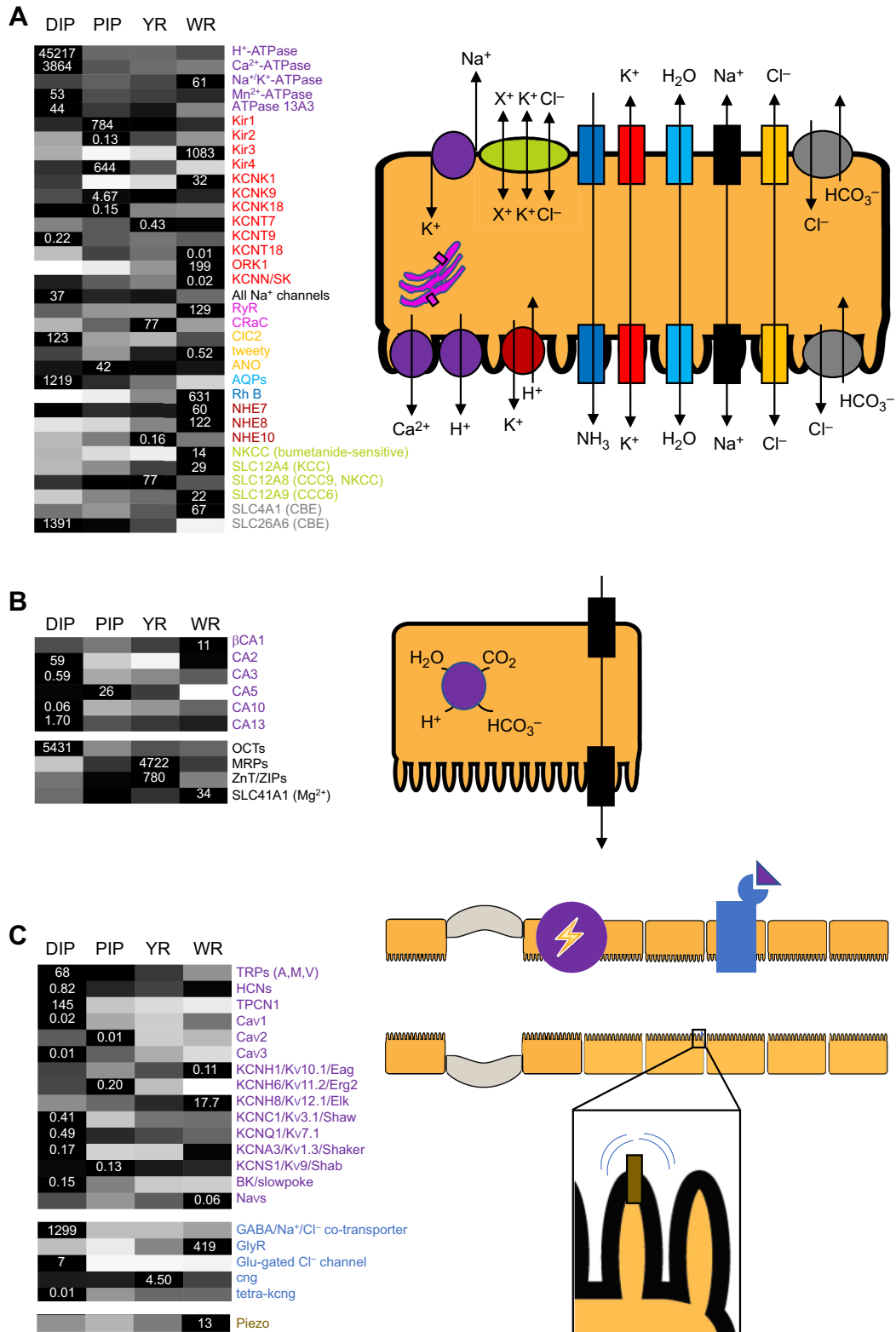
Fig. 4. Normalized heatmaps of regional ion transport transcript expression in the Malpighian tubule of larval *T. ni*. Normalized regional expression level of transcripts identified as ion transporters in the DIP, PIP, YR and WR of larval *T. ni* using RNAseq methodology. All data in normalized heatmaps are presented as average values of three biological replicates expressed in transcripts per kilobase million (TPM) and normalized to the region with the highest expression of the transcript. (A) Ion-motive ATPases, ion channels, exchangers and co-transporters, as well as aquaporins and ammonium transporters. (B) Carbonic anhydrases, xenobiotic and metal transporters. (C) Voltage-gated, ligand-gated ion channels and transporters, as well as mechanosensitive ion channel Piezo. Scales of grey are indicative of normalized regional expression, from white (i.e. 0) to black (i.e. 1=highest regional expression). Numbers in the darkest boxes indicate absolute normalized transcript abundance expressed in TPM used to illustrate absolute as well as regional abundance. Transcript IDs associated with data points in this figure are provided in Table S5. Conceptual diagrams in each panel visually summarize molecular components found in the heat map.

positive (Fig. 1E), cations must be actively secreted into the lumen of the RC MTs (Fig. 1B), likely by previously reported transporters VA, NKA, NKCC, NHA-2 and NHE-7/8 (Kolosov et al., 2018b).

Free MT: regional differences in ultrastructure, ion transport mechanisms and regulation, and putative function of the segment

The DE between adjacent regions of the free MT is pronounced (~1000–2000 DE transcripts; P_{adj}<0.05), indicating substantial differences in function (summarized in Table 2 and Fig. 7). By comparison, there are ~100–400 DE transcripts in the DIP in response to large-scale changes in dietary content of Na^+ or K^+ (Kolosov et al., 2019a).

DIP

Research to date suggests that DIP can secrete K^+, Cl^- and water, while reabsorbing Na^+, and that it serves an important function in base recovery. In the present study, the DIP was characterized by highly infolded apical membrane comprised of microvilli with individually embedded mitochondria (Fig. 2A,A′) and enrichment in ATP production, VA transport and K^+ channel activity (Table 1), higher TEP and abundant expression of organic cation transporters (Fig. 4B, Table 2).

Luminal $[K^+]$ did not alter across the entire length of the free MT (Fig. 1B). This is likely because water closely follows secretion and reabsorption of K^+ in the free MT, consistent with aquaporin expression across the MT (Fig. 4A, Table 2). In contrast to $[K^+]$, an increase in luminal $[Na^+]$ is observed across the ileac plexus (DIP→PIP), coinciding with expression of numerous Na^+ channels (Fig. 4A, Table 2) and consistent with previous reports of Na^+ transport (Irvine, 1969; O'Donnell and Ruiz-Sanchez, 2015; Kolosov et al., 2018a). Base reabsorption is evident by decreasing luminal pH (Fig. 1C), likely aided by abundant CBEs and CAs (Fig. 4B, Table 2). This indicates that base absorbed from the gut by the RC is secreted into RC MT lumen (see above), and finally reabsorbed into the haemolymph by the free MT (Moffett, 1994).

Curiously, PCs of the DIP either secrete or reabsorb K^+, depending on dietary ion content and reliant on VA, NKA, CCC9 and Kir1 (O'Donnell and Ruiz-Sanchez, 2015; Kolosov et al., 2018a,b). Our data suggest that the K^+ channels KCNK18, KCNT9 and SK may also be involved in K^+ transport – these channels, when expressed in renal epithelia demonstrate properties that may be of relevance in the MT of lepidopteran larvae – e.g. permeability to Na^+ and regulation by pH and by $[Ca^{2+}/Na^+/Cl^-]_i$ (Plant and Goldstein, 2015; Cluzeaud et al., 1998; Millar et al., 2006; Yuan et al., 2003; Ma et al., 2011; Chatelain et al., 2012). The functioning of the DIP is likely regulated by neurotransmitters, calcitonin-like diuretic hormones, Neuropeptide F and pheromone biosynthesis-activating neuropeptide (PBAN), which bind to the receptors expressed at higher levels in the DIP (Fig. 6A, Table 2) (Zandawala, 2012; Nässel and Wegener, 2011; Brighton et al., 2004; Ma et al., 2016; Elphick et al., 2018; Kawai et al., 2014). Stimulation of the DIP with above-mentioned hormones and the use of pharmacological blockers will help future studies to distinguish between mechanisms of K^+ secretion and K^+ reabsorption.

The DIP exhibited the most diverse and abundant ensemble of VGICs (Table 2). Pharmacological inhibition of one of these, HCN, resulted in PCs of the DIP switching from K^+ secretion to K^+ reabsorption (Fig. 5A). HCN, Ca_V, TRP and K_V channels have been detected in renal epithelia of vertebrates and invertebrates (Bolívar et al., 2008; Carrisoza-Gaytán et al., 2011; MacPherson et al., 2001; Grunnet et al., 2003; Chintapalli et al., 2013). Ca_V, TRP and TPCN

respond to osmotic stress and Ca^{2+} signalling (Siroky et al., 2017; Zhu et al., 2010), and HCN and K_V can alter polarization of epithelial membrane in response to cAMP and Ca^{2+} signalling, as well as extracellular $[K^+]$ (Abbott, 2014; Bleich and Warth, 2000; Demolombe et al., 2001; Morera et al., 2015; Nilius and Droogmans, 2001; Yang and Cui, 2015). However, the role of many VGICs in non-excitable tissues has not been studied to date.

Abundance and diversity of LGICs were additional hallmarks of the DIP. Stimulation with GABA altered ion transport consistent with the presence of Na^+/Cl^-/GABA co-transporter and a metabotropic GABA receptor (Figs 4C and 6A). GABA transporter was upregulated in the DIP of larvae fed ion-rich diets, where a reduction in K^+ secretion by the PCs similar to the one observed in the present study took place (Kolosov et al., 2019a).

To determine whether the above-mentioned ion channels and transporters are expressed in PCs or SCs will require further study, but it is worth noting that PCs and SCs of lepidopteran larvae demonstrate expression of Cut and Ttp transcription factors seen in the dipteran tubule (Fig. 6C), confirming their conserved developmental origin (Denholm et al., 2013). However, SCs of lepidopteran larvae are different in their ion transport properties from the SCs of other insects (O'Donnell and Ruiz-Sanchez, 2015; Kolosov et al., 2018a,b, 2019b; Kolosov and O'Donnell, 2019a,b). Cell-specific ion flux measurements and cell separation techniques will help determine whether the above-mentioned transporters are associated with a particular cell type.

PIP

In contrast to the DIP, the PIP consists mostly of PCs, and reabsorbs K^+, while secreting Na^+ and Cl^- (O'Donnell and Ruiz-Sanchez, 2015; Kolosov and O'Donnell, in press). The PIP was characterized by convoluted basolateral membrane with extensive vesicular traffic (Fig. 2B) and lower TEP. According to RNAseq data, Kir2, Kir4 and KCNK9 K^+ channels may be important for K^+ reabsorption in the PIP. In MTs of insects, Kir channels play a prominent role in K^+ secretion (Piermarini et al., 2015; Wu et al., 2015; Kolosov et al., 2018b). In contrast, the role of Kir channels in K^+ reabsorption in the MTs has not been studied. KCNK9 is a pH-dependent leak K^+ channel; extracellular acidic pH inhibits its currents (Chapman et al., 2000). A possible function for this channel is coordinating reabsorption of base and K^+.

K^+ reabsorption in the PIP may be regulated by Ast-A and the NOS/cGMP/PKG pathway. Ast-A has been demonstrated to alter K^+ transport in the insect gut (Vanderveken and O'Donnell, 2014; Robertson et al., 2014a,b). Moreover, Ast-A receptor was downregulated in the DIP of salt-fed *T. ni* larvae, coinciding with a reduction in K^+ secretion (Kolosov et al., 2019a). NO signalling in the MTs of *Aedes aegypti* has been connected with the antidiuretic action of CAPA, which acts through the NOS/cGMP/PKG pathway to suppress cAMP-mediated diuretic effects of serotonin and DH_{31} (Sajadi et al., 2018). Dissection of the role NO signalling may play in K^+ reabsorption in the PIP will proceed with the help of pharmacological blockers and SIET.

Additionally, the present study revealed that the PIP is likely to play a major role in the transport of the metal ions Zn^{2+} and Mg^{2+}, as well as trace elements present in insect diet (O'Donnell, 2008; Landry et al., 2019) and Fe^{3+}, which can be transported by Zn^{2+} transporters in *Drosophila* and mammals (Wang et al., 2012; Xiao et al., 2014; Xu et al., 2019). Lastly, the present study suggests that the PIP, YR and WR may play an important role in xenobiotic clearance and sugar reabsorption, in addition to the DIP as previously postulated (Labbe et al., 2011; O'Donnell and Ruiz-Sanchez, 2015; Kolosov et al., 2019a). Contrasting the expression
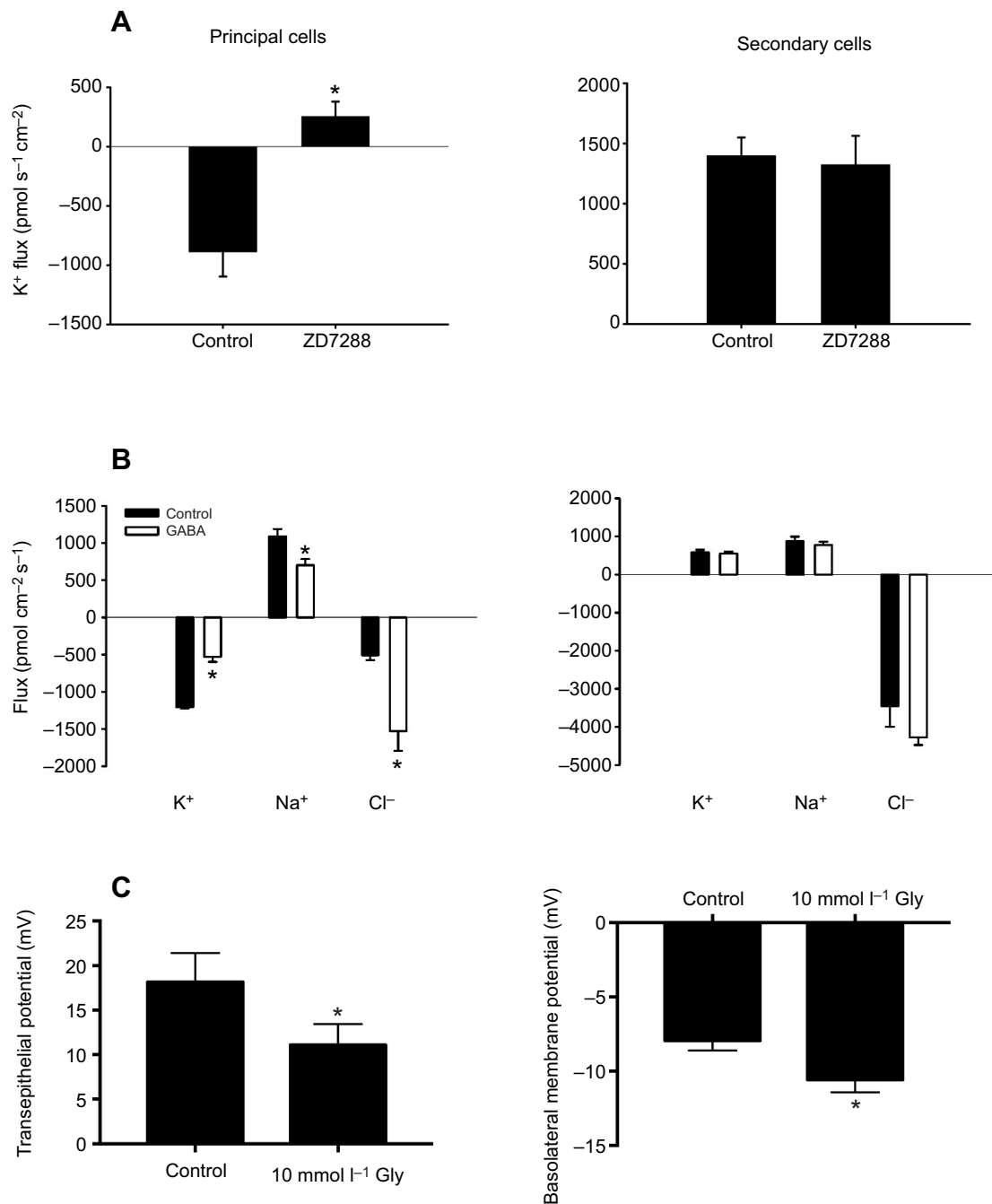
Fig. 5. Effects of voltage-gated ion channel inhibition and stimulation of ligand-gated transporters on ion transport in the Malpighian tubule of larval *T. ni*. (A) Pharmacological inhibition of HCN channels with 10 µmol l^{-1} of ZD7288 results in principal cells (PCs) of the DIP switching from K$^+$ secretion to K$^+$ reabsorption, without affecting K$^+$ reabsorption by the secondary cells (SCs). (B) Application of 1 mmol l^{-1} gamma-aminobutyric acid (GABA) to the DIP preparations resulted in reduced K$^+$ secretion, reduced Na$^+$ reabsorption and increased Cl$^-$ secretion by the PCs, without affecting ion transport by the SCs. (C) Application of 1 mmol l^{-1} glycine to the white region of the tubule resulted in reduced transepithelial potential and reduced basolateral membrane potential. All data are means±s.e.m. (N=5–8). Asterisks denote a significant difference as determined by a paired Student's *t*-test (*P<0.05).

levels of xenobiotic transporters in larvae fed plant-based and artificial diets will aid assessment of the roles of these transporters in xenobiotic clearance in future studies.

YR

In the YR, K$^+$ and Na$^+$ are reabsorbed, while Cl$^-$ is secreted in exchange for bicarbonate (O'Donnell and Ruiz-Sanchez, 2015; Kolosov 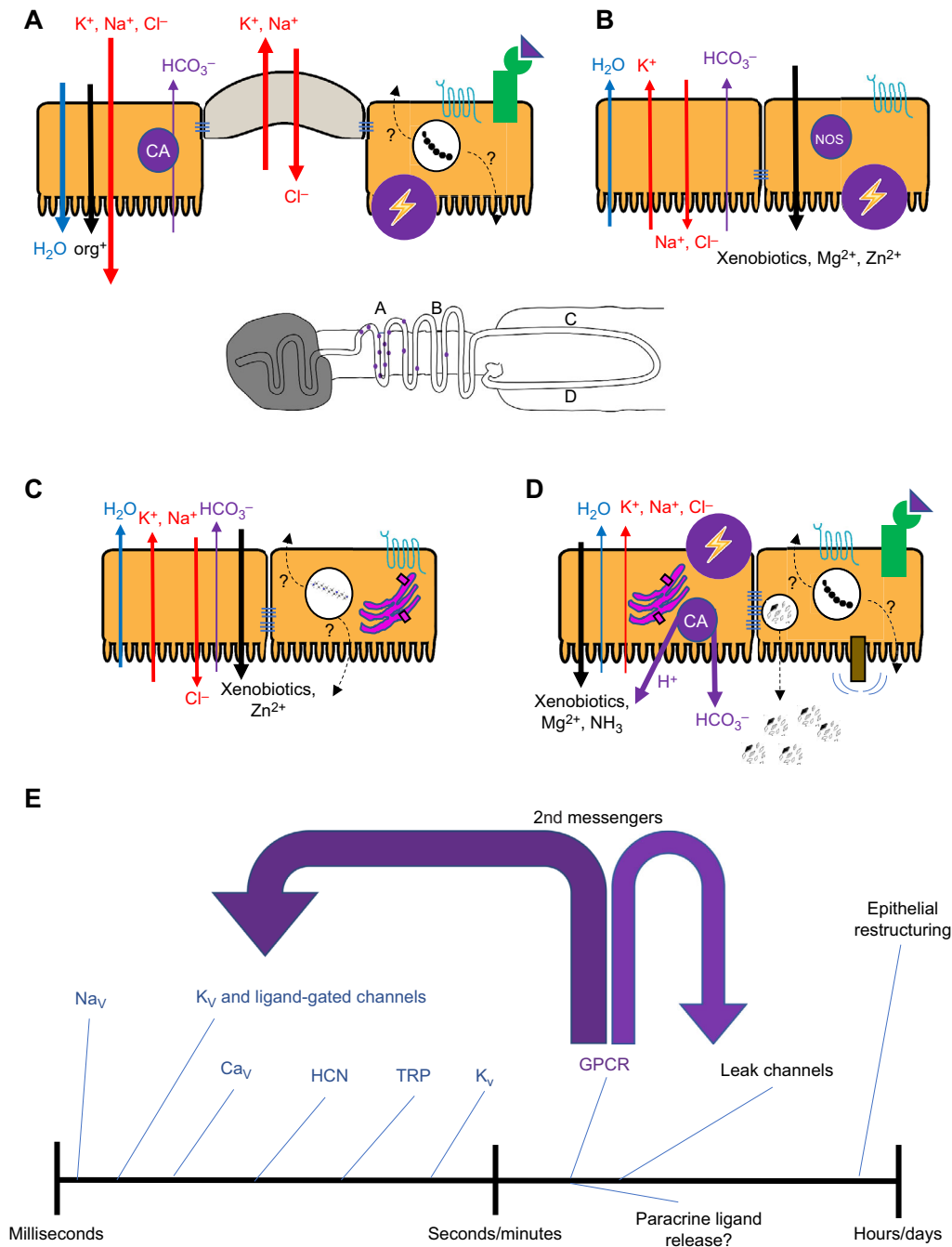and O'Donnell, in press). The YR was characterized by an extensive vesicular network adjacent to the basolateral membrane, increased TEP and abundant expression of Zn^{2+} transporters (Fig. 4B). Because luminal [K$^+$] and [Na$^+$] do not change in the YR and WR, water is likely reabsorbed as well across these regions (Fig. 1). The KCNT7 K$^+$ channel and NHE10 may play important roles in K$^+$/Na$^+$ reabsorption observed in the YR (Yuan et al., 2003; Kang'ethe et al., 2007; Piermarini et al., 2009; Pullikuth et al., 2006; Kolosov et al., 2018b).
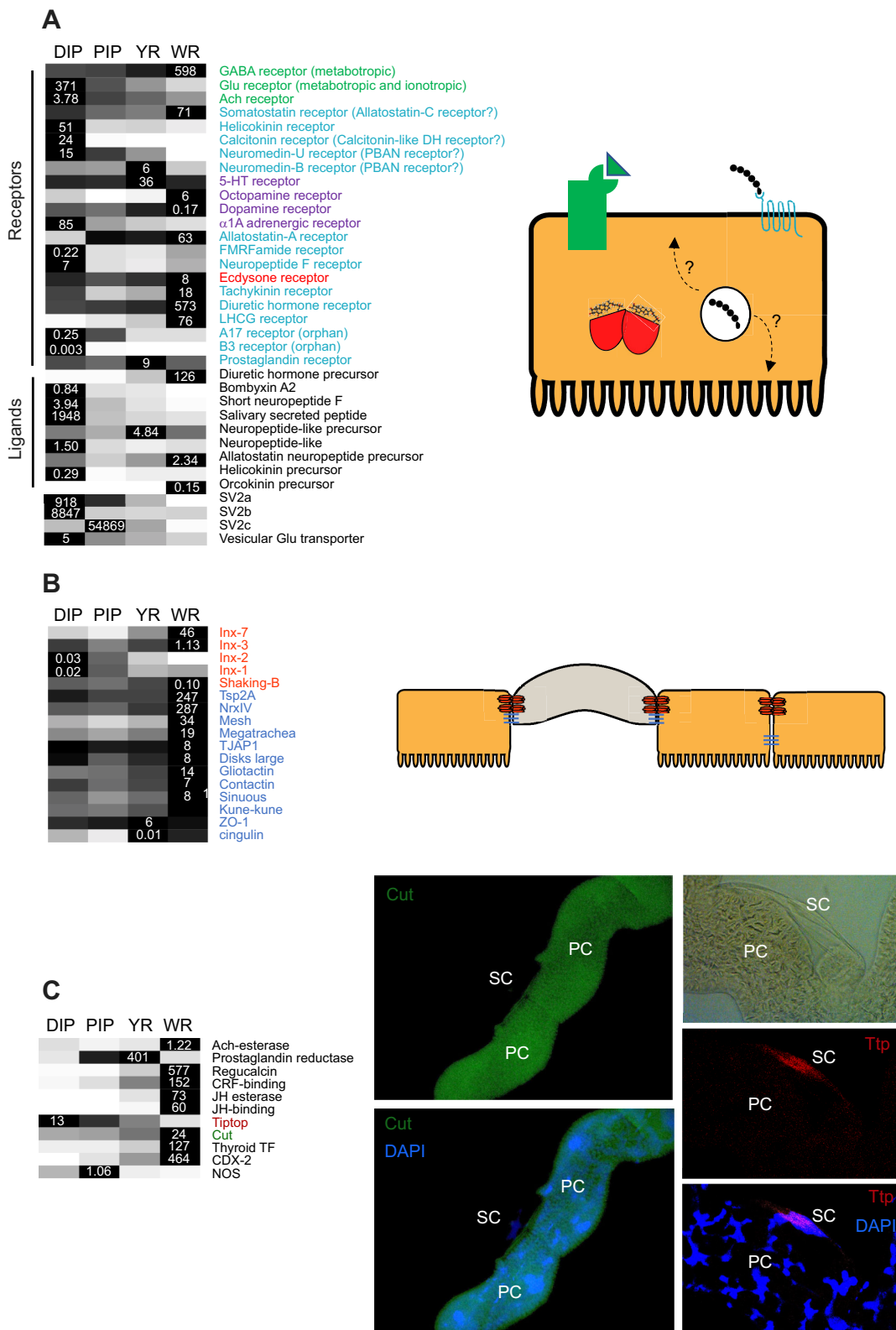
Fig. 6. Normalized heatmaps of regional regulatory transcript expression in the Malpighian tubule of larval *T. ni*. Normalized regional expression level of transcripts identified as regulatory transcripts of interest in the DIP, PIP, YR and WR of larval *T. ni* using RNAseq methodology. All data in normalized heatmaps are presented as average values of three biological replicates expressed in TPM and normalized to the region with the highest expression of the transcript. (A) Endocrine receptors, ligands and vesicle proteins. (B) Gap junction and septate junction components. Conceptual diagrams in A and B visually summarize molecular components found in the heat maps. (C) Ligand-processing components, transcription factors and nitric oxide synthase. Scales of grey are indicative of normalized regional expression, from white (i.e. 0) to black (i.e. 1=highest expression). Numbers in the darkest boxes indicate absolute normalized transcript abundance expressed in TPM used to illustrate absolute as well as regional abundance. Transcript IDs associated with data points in this figure are provided in Table S5.

Table 2. Summary of regional heterogeneity of transport properties, expression of ion and water transporters, cell–cell junctions, as well as functional specialization and possible regulatory mechanisms in the distal ileac plexus (DIP), proximal ileac plexus (PIP), yellow region (YR) and white region (WR) of Malpighian tubules of larval *T. ni*

Region	Ion and fluid transport	Transporters implicated	Junctional makeup	Functional specialization	Cellular regulatory mechanisms	Endocrine regulatory mechanisms
DIP	K^+: secretes (can reabsorb)	VA, NKA, slc12a8 (CCC9), Kir1, NHE7, KCNK18, KCNT9, SK	Gap junction: Inx-1, Inx-2	• VA-driven K^+ secretion • Acid/base balance and base reabsorption • Organic cation transport	• $[Ca^{2+}]_i$ signalling • cyclic nucleotides (e.g. Smoothened, cAMP, tetra-kcng) • Ligand-gated ion transporters (glutamate and GABA) • Voltage-gated channels (Ca_V1, Ca_V3, TRPs, HCN, TPCN1, KCNC1, KCNQ1, KCNA3, BK)	Receptors: Glu_{met}, Glu_{ion}, Ach, helicokinin, calcitonin, PBAN?, $\alpha1A$ adrenergic, FMRFamide, neuropeptide F Orphan GPCRs: A17, B3
	Na^+: reabsorbs (can secrete)	NKA, Na^+ channels, CCC9				
	Cl^-: secretes (can reabsorb)	ClC2, slc26a6 (CBE), CCC9	Septate junction: Tsp2A and Disks large			
	HCO_3^-: reabsorbs	slc26a6 (CBE), CA2, CA3, CA5, CA10, CA13				
	Water: secretes	AQPx1, AQPx2, AQP-Gra2				Ligands: Bombyxin A2, short neuropeptide F, helicokinin
PIP	K^+: reabsorbs	Kir2, Kir4, KCNK9, slc12a8 (CCC9)	—	• Zn^{2+}/Mg^{2+} transport • Xenobiotic transport and metabolism • Carbohydrate metabolism • Immune response	• Voltage-gated channels (Ca_V2, KCNH6, KCNQ1) • Nitric oxide	Receptors: Ast-A
	Na^+: secretes	Na^+ channels				Ligands: none
	Cl^-: secretes	slc26a6 (CBE), CCC9				Ligand processing: prostaglandin reductase
	HCO_3^-: reabsorbs	slc26a6 (CBE), CA5				
	Water: ?	AQPx2, AQP-Gra2				
YR	K^+: reabsorbs (can secrete)	KCNT7	—	• Zn^{2+} transport • Xenobiotic transport (MRPs) and metabolism • Amino acid transport • Polyamine biosynthesis • Immune response	• Ca^{2+}-release-activated Ca^{2+} channels (CRaC)	Receptors: Ast-A, $GABA_{met}$, PBAN?, prostaglandin
	Na^+: reabsorbs	NHE10, Na^+ channels				Ligands: neuropeptide-like precursor
	Cl^-: secretes (can reabsorb)	slc26a6 (CBE), slc4a1 (CBE), tweety (ClC)				
	HCO_3^-: ?	slc26a6 (CBE), slc4a1 (CBE)				Ligand processing: prostaglandin reductase
	Water: reabsorbs (can secrete)	AQPx2, AQP-Bom2				
WR	K^+: reabsorbs	NKA, KCC, CCC6, Kir3, KCNK1, KCNT7, ORK, NKA, NKCC, NHE8	Gap junction: Inx-3, Inx-7, Shaking-B	• Mg^{2+} transport • Xenobiotic transport • NKA-driven ion transport • Ammonium transport • Flow feedback • Restriction of water and solute back-flux • Ligand processing	• Ca^{2+}-release-activated Ca^{2+} channels (RyR) • Mechanosensation of fluid flow (Piezo) • Ligand-gated ion channels (GlyR) – voltage-gated channels (Na_V, KCNA3, KCNH1, KCNH8)	Receptors: Ast-A, $GABA_{met}$, somatostatin (=Ast-C?), octopamine, dopamine, tachykinin, DH, LCGH, ecdysone
	Na^+: reabsorbs	slc4a1 (CBE), tweety (ClC), NKCC, KCC, CCC6	Septate junction: higher expression of all transcripts – a 'tighter' epithelium?			
	Cl^-: reabsorbs					
	HCO_3^-: transports into lumen	βCA1, CA2, CA13				Ligands: DH, orcokinin, allatostatin
	Water: reabsorbs	AQP-Bom2				Ligand processing: CRF, JH, Ach

Fig. 7. Proposed model for ion transport mechanisms and regional functional specialization in the Malpighian tubule of larval _T. ni_. (A) DIP secretes K^+, Na^+, Cl^-, water and organic cations, while reabsorbing HCO_3^- – these processes are regulated by neurotransmitters (e.g. GABA), neuropeptides (e.g. helicokinin) and voltage-gated ion channels (e.g. HCN). The DIP also likely produces autocrine/paracrine peptide ligands (e.g. helicokinin). (B) As the fluid moves through the PIP, K^+, water and HCO_3^- are reabsorbed, while Na^+, Cl^-, Mg^{2+}, Zn^{2+} and xenobiotics are secreted. PIP participates in prostaglandin clearance. These processed are likely regulated by neuropeptide Ast-A and voltage-gated ion channels. Nitric oxide-dependent signalling pathways are likely to be involved in the regulation of the function of PIP. (C) As the fluid moves through the YR, K^+, Na^+, water and HCO_3^- are reabsorbed, while Cl^-, Zn^{2+} and xenobiotics are secreted into the lumen. The YR transports amino acids and participates in polyamine biosynthesis and clearing prostaglandins, and responds to their levels. The function of the YR is regulated by neuropeptides (e.g. Ast-A) and prostaglandins, and Ca^{2+} release-activated signalling pathways are likely to be involved. (D) Lastly, as the fluid moves into the last WR, K^+, Na^+, Cl^- and water are reabsorbed, while xenobiotics and Mg^{2+} continue to be secreted into the lumen. Distinctly different carbonic anhydrase makeup may contribute to ammonia trapping via Rh B transporters and deacidification of the lumen. Distinctly different gap junction and septate junction makeup suggest that intercellular communication and paracellular permeability in the WR are distinctly different from the upstream regions. The WR may be mechanosensitive to fluid flow, and when the lumen fills up with uric acid crystals and fluid flow is reduced, the WR may release endocrine ligands (e.g. DH, orcokinin and Ast-A) to provide fluid flow feedback to the renal and gut tissues. This region of the tubule is functionally regulated by neurotransmitters (e.g. GABA and glycine), neuropeptides (e.g. Ast-A and -C), amines (e.g. dopamine), steroids (e.g. ecdysone), and voltage-gated, ligand-gated and mechanosensitive ion channels. Similar to the PIP and YR, the WR may also contribute to ligand processing. (E) It appears that by employing fast response and slow response molecular machinery, ranging from voltage- and ligand-gated ion channels, in addition to conventional G protein-coupled receptor (GPCR) and second messenger pathways, the MT of larval lepidopterans is capable of quickly readjusting its function, depending on its luminal content and membrane potential. It appears that paracrine release and epithelial restructuring may also play a role in how the tubule autoregulates its function.

The YR demonstrated enrichment in transcripts associated with xenobiotic and carbohydrate metabolism (Table 1), including high levels of Tret1 and MRP expression (Table S5, Sugar transport). The YR may also participate in biosynthesis of polyamines, which trigger protein phosphorylation in a manner distinct from Ca^{2+} and cAMP second messengers, altering RNA and protein synthesis (Birnbaum et al., 1988). In lepidopterans, polyamines have been shown to be produced in the brain and the fat body, where ornithine decarboxylase activity declines precipitously in both tissues as the fifth instar larva feeds and grows (Birnbaum et al., 1988). It is possible that polyamine biosynthesis is subsequently shifted to the renal tissues. Interestingly, ecdysone stimulates ornithine decarboxylase activity in MTs of *Drosophila*, linking growth/ moulting and renal function (Birnbaum and Gilbert, 1990). Tracking expression of ornithine decarboxylase in the YR throughout development should help establish whether the renal tissue in larvae participates in biosynthesis of polyamines.

Ion transport and metabolism in the YR are likely regulated by dopamine, $GABA_{met}$, PBAN and prostaglandins. Dopamine and prostaglandins are known to modulate fluid secretion rate in insect epithelia, while prostaglandins additionally play an important role in immune responses (Nicolson and Millar, 1983; Morgan and Mordue, 1984; Kim et al., 2014; Petzel et al., 1993; Ahmed et al., 2019; Stanley and Kim, 2019; Dow and Davies, 2006; Davies et al., 2012).

WR

The WR is characterized by reabsorption of Na^+, K^+ and Cl^- (O'Donnell and Ruiz-Sanchez, 2015; Kolosov and O'Donnell, submitted). In the present study, the WR demonstrated what appears to be transepithelial vesicular traffic, a lower TEP and higher luminal pH. Higher luminal pH and a distinctly different combination of CBE and CA transcripts in the WR (Figs 1C, 4A,B) likely contribute HCO_3^- for acid–base balance, and H^+ for ammonia trapping and uric acid precipitation in intracellular vesicles (Haley and O'Donnell, 1997; Weihrauch et al., 2012).

K^+ reabsorption may be enabled by the combination of an inward rectifier Kir3 and an outward rectifier ORK1 (Piermarini et al., 2015; Goldstein et al., 1996), as well as KCNK1 and KCNT18. We also suggest that NKA, NHE8, NKCC, KCC and CCC6 cotransporters play a role in reabsorption of Na^+, K^+ and Cl^-. It is worth noting that NKA, NHE8 and a different CCC9 have also been reported in the secretory DIP segment of *T. ni* tubules (Kolosov et al., 2018b, 2019a). However, in contrast to the DIP, the WR shows decreased abundance of VA transcripts, but enriched expression of NKA. If we assume that the CCC6 is apical in the WR, this arrangement of transporters, and the absence of VA, would allow the basolateral NKA to energize reabsorption (Epstein et al., 1983). The expression of several different CCCs is of special interest in light of recent work demonstrating that CCCs in *A. aegypti* may have diverged to play distinct roles in ion secretion and reabsorption (Piermarini et al., 2017).

WR function may be regulated by delayed rectifier KCNH channels (Shi et al., 1997; Schönherr et al., 2000) and Na_V channels, which are implicated in physiology and pathophysiology of vertebrate epithelia (Barshack et al., 2008; House et al., 2010). The region is also likely to be sensitive to glycine and mechanosensation of the fluid flow, mediated by GlyR and Piezo (Peyronnet et al., 2013). The WR regularly fills up with uric acid crystals (Cheung and Wang, 1994) and drains into the bladder, which empties periodically – this may create variable pressure and fluid flow. Future studies employing luminal perfusions, Piezo

blockers and electrophysiology will help deduce how this mechanosensitive ion channel contributes to renal function in lepidopteran larvae.

The WR also shows the highest expression levels of receptors for diuretic hormone, octopamine, tachykinin, somatostatin (likely binds Ast-C in insects; Elphick et al., 2018) and LHCG, and similar GABA receptor levels to the YR. Many of these ligands are diuretic and myoinhibitory (Audsley et al., 2008; Mayoral et al., 2010; Skaer et al., 2002; Nicolson and Millar, 1983; Cady and Hagedorn, 1999; Coast et al., 2005; Halberg et al., 2015). However, their effects on reabsorptive segments of the MT remain unstudied to date.

Expression of cell–cell junction components

The present study revealed notable proximo-distal (WR→DIP) heterogeneity in the expression of gap junction and septate junction components. The DIP of *T. ni* is composed of two cell types (PCs and SCs) that are coupled by gap junctions, which are thought to partially enable SC-based cation reabsorption (Kolosov et al., 2018a; Kolosov and O'Donnell, 2019b). In general, permeability properties (e.g. gating, selectivity, rectification) of the invertebrate gap junction are largely dictated by its molecular components (Skerrett and Williams, 2016). Thus, our results suggest that PC–PC gap junction in the WR may differ in its properties from the SC–PC gap junction in the DIP.

Higher expression levels of septate junction components in the WR indicate that paracellular permeability in this region may be distinctly different from that in the upstream regions. Septate junction physiology has been shown to be important for the understanding of MT function in larval Lepidoptera, which regulate paracellular permeability of their MTs together with ion transport and water permeability (Kolosov et al., 2019b). Study of molecular components of gap junctions and septate junctions should prove fruitful in the years to come.

Expression of peptide ligand precursors and processing of endocrine ligands in the free MT of lepidopteran larvae

Expression of peptide ligand precursors and ligand-processing enzymes suggests possible autocrine/paracrine regulation of ion transport in the MTs and, possibly, processing of endocrine ligands. The fluid secretion rate of isolated MTs of *Drosophila* was reported to be stimulated by an unknown diuretic factor found in the secreted fluid (Riegel et al., 1999). Because of the loop in the free MT along the midgut, the relative proximity between the WR and the DIP makes autonomous feedback, analogous to tubule–glomerular feedback in the vertebrate kidney, all the more plausible. In addition to affecting ion transport, several ligands expressed in MTs are known to affect contraction of the gut (Veenstra et al., 2008; Vanderveken and O'Donnell, 2014; Pascual et al., 2004; Hofer et al., 2005; Hofer and Homberg, 2006; Yamanaka et al., 2010; Wulff et al., 2017). Ligands released by the WR as a part of its mechanosensation of reduced fluid flow may alter motility of the gut (e.g. contraction of the RC) and ion transport in the rectum and subsequent diuresis of the secretory RC MTs and DIP. Moreover, the effects of produced ligands may extend past the digestive tract, targeting ecdysone production by the prothoracic gland and carbohydrate metabolism in the larvae (Iwami, 2000; Kawabe et al., 2019).

References

Abbott, G. W. (2014). Biology of the KCNQ1 potassium channel. *New J. Sci.* **2014**, 1-26. doi:10.1155/2014/237431

Ahmed, S., Hasan, A. and Kim, Y. (2019). Overexpression of PGE_2 synthase by in vivo transient expression enhances immunocompetency along with fitness cost in a lepidopteran insect. *J. Exp. Biol.* **222**, jeb207019. doi:10.1242/jeb.207019

Audsley, N., Coast, G. M. and Schooley, D. A. (1993). The effects of *Manduca sexta* diuretic hormone on fluid transport by the Malpighian tubules and cryptonephric complex of *Manduca sexta*. *J. Exp. Biol.* **178**, 231-243.

Audsley, N., Matthews, H. J., Price, N. R. and Weaver, R. J. (2008). Allatoregulatory peptides in Lepidoptera, structures, distribution and functions. *J. Insect Physiol.* **54**, 969-980. doi:10.1016/j.jinsphys.2008.01.012

Barry, P. H. and Lynch, J. W. (1991). Liquid junction potentials and small cell effects in patch-clamp analysis. *J. Membr. Biol.* **121**, 101-117. doi:10.1007/BF01870526

Barshack, I., Levite, M., Lang, A., Fudim, E., Picard, O., Ben Horin, S. and Chowers, Y. (2008). Functional voltage-gated sodium channels are expressed in human intestinal epithelial cells. *Digestion* **77**, 108-117. doi:10.1159/000123840

Berenbaum, M. (1980). Adaptive significance of midgut pH in larval Lepidoptera. *Am. Naturalist* **115**, 138-146. doi:10.1086/283551

Birnbaum, M. J. and Gilbert, L. I. (1990). Juvenile hormone stimulation of ornithine decarboxylase activity during vitellogenesis in *Drosophila melanogaster*. *J. Comp. Physiol. B Biochem. Sys. Environ. Physiol.* **160**, 145-151. doi:10.1007/BF00300946

Birnbaum, M. J., Whelan, T. M. and Gilbert, L. I. (1988). Temporal alterations in polyamine content and ornithine decarboxylase activity during the larval-pupal development of *Manduca sexta*. *Insect Biochem.* **18**, 853-859. doi:10.1016/0020-1790(88)90110-2

Bleich, M. and Warth, R. (2000). The very small-conductance K^+ channel KVLQT1 and epithelial function. *Pflügers Arch. Euro. J. Physiol.* **440**, 202-206. doi:10.1007/s004240000257

Bolívar, J. J., Tapia, D., Arenas, G., Castañón-Arreola, M., Torres, H. and Galarraga, E. (2008). A hyperpolarization-activated, cyclic nucleotide-gated, (Ih-like) cationic current and HCN gene expression in renal inner medullary collecting duct cells. *Am. J. Physiol. Cell Physiol.* **294**, C893-C906. doi:10.1152/ajpcell.00616.2006

Brighton, P. J., Szekeres, P. G. and Willars, G. B. (2004). Neuromedin U and its receptors: structure, function, and physiological roles. *Pharmacol. Rev.* **56**, 231-248. doi:10.1124/pr.56.2.3

Cady, C. and Hagedorn, H. H. (1999). Effects of putative diuretic factors on intracellular second messenger levels in the Malpighian tubules of *Aedes aegypti*. *J. Insect Physiol.* **45**, 327-337. doi:10.1016/S0022-1910(98)00130-9

Carrisoza-Gaytán, R., Rangel, C., Salvador, C., Saldaña-Meyer, R., Escalona, C., Satlin, L. M., Liu, W., Zavilowitz, B., Trujillo, J., Bobadilla, N. A. et al. (2011). The hyperpolarization-activated cyclic nucleotide-gated HCN2 channel transports ammonium in the distal nephron. *Kid. Intl.* **80**, 832-840. doi:10.1038/ki.2011.230

Chapman, C. G., Meadows, H. J., Godden, R. J., Campbell, D. A., Duckworth, M., Kelsell, R. E., Murdock, P. R., Randall, A. D., Rennie, G. I. Gloger, I. S. (2000). Cloning, localisation and functional expression of a novel human, cerebellum specific, two pore domain potassium channel. *Mol. Brain Res.* **82**, 74-83. doi:10.1016/S0169-328X(00)00183-2

Chatelain, F. C., Bichet, D., Douguet, D., Feliciangeli, S., Bendahhou, S., Reichold, M., Warth, R., Barhanin, J. and Lesage, F. (2012). TWIK1, a unique background channel with variable ion selectivity. *Proc. Natl. Acad. Sci. USA* **109**, 5499-5504. doi:10.1073/pnas.1201132109

Cheung, W. W.-K. and Wang, J.-B. (1994). Functional differentiation in the malpighian tubules of *Pieris canidia* (Lepidoptera: Pieridae) larva: a histochemical study. *Ann. Entomol. Soc. Am.* **87**, 901-907. doi:10.1093/aesa/87.6.901

Chintapalli, V. R., Wang, J., Herzyk, P., Davies, S. A. and Dow, J. A. T. (2013). Data-mining the FlyAtlas online resource to identify core functional motifs across transporting epithelia. *BMC Genomics* **14**, 518. doi:10.1186/1471-2164-14-518

Cluzeaud, F., Reyes, R., Escoubet, B., Fay, M., Lazdunski, M., Bonvalet, J. P., Lesage, F. and Farman, N. (1998). Expression of TWIK-1, a novel weakly inward rectifying potassium channel in rat kidney. *Am. J. Physiol.* **275**, C1602-C1609. doi:10.1152/ajpcell.1998.275.6.C1602

Coast, G. M., Garside, C. S., Webster, S. G., Schegg, K. M. and Schooley, D. A. (2005). Mosquito natriuretic peptide identified as a calcitonin-like diuretic hormone in *Anopheles gambiae* (Giles). *J. Exp. Biol.* **208**, 3281-3291. doi:10.1242/jeb.01760

Davies, S.-A., Overend, G., Sebastian, S., Cundall, M., Cabrero, P., Dow, J. A. T. and Terhzaz, S. (2012). Immune and stress response 'cross-talk' in the Drosophila Malpighian tubule. *J. Insect Physiol.* **58**, 488-497. doi:10.1016/j.jinsphys.2012.01.008

Davies, S. A., Cabrero, P., Marley, R., Corrales, G. M., Ghimire, S., Dornan, A. J. and Dow, J. A. (2019). Epithelial function in the *Drosophila* Malpighian tubule: an in vivo renal model. In *Kidney Organogenesis* (ed. S. Vainio), pp. 203-221. New York: Humana Press.

Dawkar, V. V., Chikate, Y. R., Lomate, P. R., Dholakia, B. B., Gupta, V. S. and Giri, A. P. (2013). Molecular insights into resistance mechanisms of lepidopteran insect pests against toxicants. *J. Proteome Res.* **12**, 4727-4737. doi:10.1021/pr400642p

Demolombe, S., Franco, D., de Boer, P., Kuperschmidt, S., Roden, D., Pereon, Y., Jarry, A., Moorman, A. F. and Escande, D. (2001). Differential expression of KvLQT1 and its regulator IsK in mouse epithelia. *Am. J. Physiol. Cell Physiol.* **280**, C359-C372. doi:10.1152/ajpcell.2001.280.2.C359

Denholm, B., Hu, N., Fauquier, T., Caubit, X., Fasano, L. and Skaer, H. (2013). The tiptop/teashirt genes regulate cell differentiation and renal physiology in *Drosophila*. *Development* **140**, 1100-1110. doi:10.1242/dev.088989

Donini, A. and O'Donnell, M. J. (2005). Analysis of Na+, Cl–, K+, H+ and NH4+ concentration gradients adjacent to the surface of anal papillae of the mosquito *Aedes aegypti*: application of self-referencing ion-selective microelectrodes. *J. Exp. Biol.* **208**, 603-610. doi:10.1242/jeb.01422

Dow, J. A. T. and Davies, S. A. (2006). The Malpighian tubule: rapid insights from post-genomic biology. *J. Insect Physiol.* **52**, 365-378. doi:10.1016/j.jinsphys.2005.10.007

Elphick, M. R., Mirabeau, O. and Larhammar, D. (2018). Evolution of neuropeptide signalling systems. *J. Exp. Biol.* **221**, jeb151092-j16. doi:10.1242/jeb.151092

Epstein, F. H., Stoff, J. S. and Silva, P. (1983). Mechanism and control of hyperosmotic NaCl-rich secretion by the rectal gland of *Squalus acanthias*. *J. Exp. Biol.* **106**, 25-41.

Fu, Y., Yang, Y., Zhang, H., Farley, G., Wang, J., Quarles, K. A., Weng, Z. and Zamore, P. D. (2018). The genome of the Hi5 germ cell line from *Trichoplusia ni*, an agricultural pest and novel model for small RNA biology. *eLife* **7**, e31628. doi:10.7554/eLife.31628

Gautam, N. K., Verma, P. and Davidson, A. J. (2017). *Drosophila* Malpighian tubules: a model for understanding kidney development, function, and disease. In *Kidney Development and Disease* (ed. R. K. Miller), pp. 3-26. Springer International Publishing.

Goecks, J., Nekrutenko, A., Taylor, J. and The Galaxy Team (2010). Galaxy: a comprehensive approach for supporting accessible, reproducible, and transparent computational research in the life sciences. *Genome Biol.* **11**, R86. doi:10.1186/gb-2010-11-8-r86

Goldstein, S. A. N., Price, L. A., Rosenthal, D. N. and Pausch, M. H. (1996). ORK1, a potassium-selective leak channel with two pore domains cloned from *Drosophila melanogaster* by expression in *Saccharomyces cerevisiae*. *Proc. Natl. Acad. Sci.* **93**, 13256-13261. doi:10.1073/pnas.93.23.13256

Gotthard, K. (2008). Adaptive growth decisions in butterflies. *Bioscience* **58**, 222-230. doi:10.1641/B580308

Grunnet, M., Rasmussen, H. B., Hay-Schmidt, A. and Klaerke, D. A. (2003). The voltage-gated potassium channel subunit, Kv1.3, is expressed in epithelia. *Biochim. Biophys. Acta Biomembr.* **1616**, 85-94. doi:10.1016/S0005-2736(03)00198-6

Halberg, K. A., Terhzaz, S., Cabrero, P., Davies, S. A. and Dow, J. A. T. (2015). Tracing the evolutionary origins of insect renal function. *Nat. Commun.* **6**, 6800. doi:10.1038/ncomms7800

Haley, C. and O'Donnell, M. (1997). K^+ reabsorption by the lower Malpighian tubule of *Rhodnius prolixus*: inhibition by Ba^{2+} and blockers of H^+/K^+-ATPases. *J. Exp. Biol.* **200**, 139-147.

Hofer, S. and Homberg, U. (2006). Evidence for a role of orcokinin-related peptides in the circadian clock controlling locomotor activity of the cockroach *Leucophaea maderae*. *J. Exp. Biol.* **209**, 2794-2803. doi:10.1242/jeb.02307

Hofer, S., Dircksen, H., Tollbäck, P. and Homberg, U. (2005). Novel insect orcokinins: characterization and neuronal distribution in the brains of selected dicondylian insects. *J. Comp. Neurol.* **490**, 57-71. doi:10.1002/cne.20650

House, C. D., Vaske, C. J., Schwartz, A. M., Obias, V., Frank, B., Luu, T., Sarvazyan, N., Irby, R., Strausberg, R. L., Hales, T. G. et al. (2010). Voltage-gated Na+ channel SCN5A is a key regulator of a gene transcriptional network that

controls colon cancer invasion. *Cancer Res.* **70**, 6957-6967. doi:10.1158/0008-5472.CAN-10-1169

Irvine, H. B. (1969). Sodium and potassium secretion by isolated insect Malpighian tubules. *Am. J. Physiol.* **217**, 1520-1527. doi:10.1152/ajplegacy.1969.217.5.1520

Iwami, M. (2000). Bombyxin: an insect brain peptide that belongs to the insulin family. *Zool. Sci.* **17**, 1035-1044. doi:10.2108/zsj.17.1035

Kang'ethe, W., Aimanova, K. G., Pullikuth, A. K. and Gill, S. S. (2007). NHE8 mediates amiloride-sensitive Na$^+$/H$^+$ exchange across mosquito Malpighian tubules and catalyzes Na+ and K+ transport in reconstituted proteoliposomes. *Am. J. Physiol. Renal Physiol.* **292**, F1501-F1512. doi:10.1152/ajprenal.00487.2005

Kawabe, Y., Waterson, H. and Mizoguchi, A. (2019). Bombyxin (bombyx insulin-like peptide) increases the respiration rate through facilitation of carbohydrate catabolism in *Bombyx mori*. *Front. Endocrinol.* **10**, 63-67. doi:10.3389/fendo.2019.00150

Kawai, T., Katayama, Y., Guo, L., Liu, D., Suzuki, T., Hayakawa, K., Lee, J. M., Nagamine, T., Hull, J. J., Matsumoto, S. et al. (2014). Identification of functionally important residues of the silkmoth pheromone biosynthesis-activating neuropeptide receptor, an insect ortholog of the vertebrate neuromedin U receptor. *J. Biol. Chem.* **289**, 19150-19163. doi:10.1074/jbc.M113.488999

Kim, D., Šimo, L. and Park, Y. (2014). Orchestration of salivary secretion mediated by two different dopamine receptors in the blacklegged tick *Ixodes scapularis*. *J. Exp. Biol.* **217**, 3656-3663. doi:10.1242/jeb.109462

Kolosov, D. and O'Donnell, M. J. (2019a). Helicokinin alters ion transport in the secondary cell-containing region of the Malpighian tubule of the larval cabbage looper *Trichoplusia ni*. *Gen. Comp. Endocrinol.* **278**, 12-24. doi:10.1016/j.ygcen.2018.07.005

Kolosov, D. and O'Donnell, M. J. (2019b). Ion transport in the Malpighian tubules of Lepidopteran larvae, In *Advances in Insect Physiology*, Vol. 56 (ed. R. Jurenka), pp. 165-202. London: Elsevier, Academic Press.

Kolosov, D. and O'Donnell, M. J. (in press). Mechanisms and regulation of chloride transport in the Malpighian tubules of the larval cabbage looper *Trichoplusia ni*. *Insect Biochem. Mol. Biol.* doi:10.1016/j.ibmb.2019.103263

Kolosov, D., Piermarini, P. M. and O'Donnell, M. J. (2018a). Malpighian tubules of *Trichoplusia ni*: recycling ions via gap junctions and switching between secretion and reabsorption of Na$^+$ and K$^+$ in the distal ileac plexus. *J. Exp. Biol.* **221**, jeb172296. doi:10.1242/jeb.172296

Kolosov, D., Tauqir, M., Rajaruban, S., Piermarini, P. M., Donini, A. and O'Donnell, M. J. (2018b). Molecular mechanisms of bi-directional ion transport in the Malpighian tubules of a lepidopteran crop pest, *Trichoplusia ni*. *J. Insect. Physiol.* **109**, 55-68. doi:10.1016/j.jinsphys.2018.06.005

Kolosov, D., Donly, C., MacMillan, H. and O'Donnell, M. J. (2019a). Transcriptomic analysis of the Malpighian tubules of *Trichoplusia ni*: clues to mechanisms for switching from ion secretion to ion reabsorption in the distal ileac plexus. *J. Insect Physiol.* **112**, 73-89. doi:10.1016/j.jinsphys.2018.12.005

Kolosov, D., Jonusaite, S., Donini, A., Kelly, S. P. and O'Donnell, M. J. (2019b). Septate junction in the distal ileac plexus of larval lepidopteran *Trichoplusia ni*: alterations in paracellular permeability during ion transport reversal. *J. Exp. Biol.* **222**, jeb204750. doi:10.1242/jeb.204750

Kümmel, G. (1973). Filtration structures in excretory systems – a comparison. In *Comparative Physiology: Locomotion, Respiration, Transport and Blood* (ed. K. Schmidt-Nielsen, L. Bolis and S. H. P. Maddrell), pp. 221-241. Amsterdam, North Holland.

Labbe, R., Caveney, S. and Donly, C. (2011). Expression of multidrug resistance proteins is localized principally to the Malpighian tubules in larvae of the cabbage looper moth, *Trichoplusia ni*. *J. Exp. Biol.* **214**, 937-944. doi:10.1242/jeb.051060

Landry, G. M., Furrow, E., Holmes, H. L., Hirata, T., Kato, A., Williams, P., Strohmaier, K., Gallo, C. J. R., Chang, M., Pandey, M. K. et al. (2019). Cloning, function, and localization of human, canine, and *Drosophila* ZIP10 (SLC39A10), a Zn^{2+} transporter. *Am. J. Physiol. Renal Physiol.* **316**, F263-F273. doi:10.1152/ajprenal.00573.2017

Liao, S., Audsley, N. and Schooley, D. A. (2000). Antidiuretic effects of a factor in brain/corpora cardiaca/corpora allata extract on fluid reabsorption across the cryptonephric complex of *Manduca sexta*. *J. Exp. Biol.* **203**, 605-615.

Love, M. I., Huber, W. and Anders, S. (2014). Moderated estimation of fold change and dispersion for RNA-seq data with DESeq2. *Genome Biol.* **15**, 550. doi:10.1186/s13059-014-0550-8

Ma, L., Zhang, X. and Chen, H. (2011). TWIK-1 two-pore domain potassium channels change ion selectivity and conduct inward leak sodium currents in hypokalemia. *Sci. Signal.* **4**, ra37. doi:10.1126/scisignal.2001726

Ma, Z., Su, J., Guo, T., Jin, M., Li, X., Lei, Z., Hou, Y., Li, X., Jia, C., Zhang, Z. et al. (2016). Neuromedin B and its receptor: gene cloning, tissue distribution and expression levels of the reproductive axis in pigs. *PLoS ONE* **11**, e0151871-e21. doi:10.1371/journal.pone.0151871

MacPherson, M. R., Pollock, V. P., Broderick, K. E., Kean, L., O'Connell, F. C., Dow, J. A. T. and Davies, S. A. (2001). Model organisms: new insights into ion channel and transporter function. L-type calcium channels regulate epithelial fluid transport in Drosophila melanogaster. *Am. J. Physiol. Cell Physiol.* **280**, C394-C407. doi:10.1152/ajpcell.2001.280.2.C394

Maddrell, S. (1981). The functional design of the insect excretory system. *J. Exp. Biol.* **90**, 1-15.

Maddrell, S. H. and Gardiner, B. O. (1976). Excretion of alkaloids by Malpighian tubules of insects. *J. Exp. Biol.* **64**, 267-281.

Marelja, Z. and Simons, M. (2019). Filling the gap: *Drosophila* nephrocytes as model system in kidney research. *J. Am. Soc. Nephrol.* **30**, 719-720. doi:10.1681/ASN.2019020181

Mayoral, J. G., Nouzova, M., Brockhoff, A., Goodwin, M., Hernandez-Martinez, S., Richter, D., Meyerhof, W. and Noriega, F. G. (2010). Allatostatin-C receptors in mosquitoes. *Peptides*, **31**, 442-450. doi:10.1016/j.peptides.2009.04.013

McMorran, A. (1965). A synthetic diet for the spruce budworm, *Choristoneura fumiferana* (Clem.) (Lepidoptera: Tortricidae). *Can. Entomol.* **97**, 58-62. doi:10.4039/Ent9758-1

Millar, I. D., Taylor, H. C., Cooper, G. J., Kibble, J. D., Barhanin, J. and Robson, L. (2006). Adaptive downregulation of a quinidine-sensitive cation conductance in renal principal cells of TWIK-1 knockout mice. *Pflugers Arch.* **453**, 107-116. doi:10.1007/s00424-006-0107-0

Millet-Boureima, C., Porras Marroquin, J. and Gamberi, C. (2018). Modeling renal disease 'on the fly'. *BioMed. Res. Intl.* **2018**, 5697436. doi:10.1155/2018/5697436

Moffett, D. F. (1994). Recycling of K$^+$, acid-base equivalents, and fluid between gut and hemolymph in lepidopteran larvae. *Physiol. Zool.* **67**, 68-81. doi:10.1086/physzool.67.1.30163835

Morera, F. J., Saravia, J., Pontigo, J. P., Vargas-Chacoff, L., Contreras, G. F., Pupo, A., Lorenzo, Y., Castillo, K., Tilegenova, C., Cuello, L. G. et al. (2015). Voltage-dependent BK and Hv1 channels expressed in non-excitable tissues: new therapeutics opportunities as targets in human diseases. *Pharmacol. Res.* **101**, 56-64. doi:10.1016/j.phrs.2015.08.011

Morgan, P. J. and Mordue, W. (1984). 5-Hydroxytryptamine stimulates fluid secretion in locust Malpighian tubules independently of cAMP. *Comp. Bichem. Physiol.* **79**, 305-310. doi:10.1016/0742-8413(84)90205-6

Nässel, D. R. and Wegener, C. (2011). A comparative review of short and long neuropeptide F signaling in invertebrates: Any similarities to vertebrate neuropeptide Y signaling? *Peptides* **32**, 1335-1355. doi:10.1016/j.peptides.2011.03.013

Neher, E. (1992). Correction for liquid junction potentials in patch clamp experiments. *Methods Enzymol.* **207**, 123-131. doi:10.1016/0076-6879(92)07008-C

Nicolson, S. W. and Millar, R. P. (1983). Effects of biogenic amines and hormones on butterfly Malpighian tubules: dopamine stimulates fluid secretion. *J. Insect Physiol.* **29**, 611-615. doi:10.1016/0022-1910(83)90012-4

Nilius, B. and Droogmans, G. (2001). Ion channels and their functional role in vascular endothelium. *Physiol. Rev.* **81**, 1415-1459. doi:10.1152/physrev.2001.81.4.1415

O'Donnell, M. (2008). Insect excretory mechanisms. In *Advances in Insect Physiology*, Vol. 35 (ed. S. J. Simpson), pp. 1-122. Elsevier, Academic Press.

O'Donnell, M. J. and Ruiz-Sanchez, E. (2015). The rectal complex and Malpighian tubules of the cabbage looper (*Trichoplusia ni*): regional variations in Na$^+$ and K$^+$ transport and cation reabsorption by secondary cells. *J. Exp. Biol.* **218**, 3206-3214. doi:10.1242/jeb.128314

O'Donnell, M. J., Rheault, M. R., Davies, S. A., Rosay, P., Harvey, B. J., Maddrell, S. H. P., Kaiser, K. and Dow, J. A. T. (1998). Hormonally controlled chloride movement across *Drosophila* tubules is via ion channels in stellate cells. *Am. J. Physiol. Regul. Integr. Comp. Physiol.* **274**, R1039-R1049. doi:10.1152/ajpregu.1998.274.4.R1039

Onken, H. and Moffett, D. F. (2017). Acid-base loops in insect larvae with extremely alkaline midgut regions. In *Acid-Base Balance and Nitrogen Excretion in Invertebrates* (ed. D. Weihrauch and M. J. O'Donnell), pp. 239-260. Springer.

Pascual, N., Castresana, J., Valero, M.-L., Andreu, D. and Bellés, X. (2004). Orcokinins in insects and other invertebrates. *Insect Biochem. Mol. Biol.* **34**, 1141-1146. doi:10.1016/j.ibmb.2004.07.005

Patro, R., Duggal, G., Love, M. I., Irizarry, R. A. and Kingsford, C. (2017). Salmon provides fast and bias-aware quantification of transcript expression. *Nat. Methods* **14**, 417-419. doi:10.1038/nmeth.4197

Petzel, D. H., Parrish, A. K., Ogg, C. L., Witters, N. A., Howard, R. W. and Stanley-Samuelson, D. W. (1993). Arachidonic acid and prostaglandin E2 in Malpighian tubules of female yellow fever mosquitoes. *Insect Biochem. Mol. Biol.* **23**, 431-437. doi:10.1016/0965-1748(93)90050-3

Peyronnet, R., Martins, J. R., Duprat, F., Demolombe, S., Arhatte, M., Jodar, M., Tauc, M., Duranton, C., Paulais, M., Teulon, J. et al. (2013). Piezo1-dependent stretch-activated channels are inhibited by Polycystin-2 in renal tubular epithelial cells. *EMBO Rep.* **14**, 1143-1148. doi:10.1038/embor.2013.170

Phillips, J. (1981). Comparative physiology of insect renal function. *Am. J. Physiol.* **241**, R241-R257. doi:10.1152/ajpregu.1981.241.5.R241

Piermarini, P. M., Weihrauch, D., Meyer, H., Huss, M. and Beyenbach, K. W. (2009). NHE8 is an intracellular cation/H$^+$ exchanger in renal tubules of the yellow fever mosquito *Aedes aegypti*. *Am. J. Physiol. Renal Physiol.* **296**, F730-F750. doi:10.1152/ajprenal.90564.2008

Piermarini, P. M., Dunemann, S. M., Rouhier, M. F., Calkins, T. L., Raphemot, R., Denton, J. S., Hine, R. M. and Beyenbach, K. W. (2015). Localization and role of inward rectifier K$^+$ channels in Malpighian tubules of the yellow fever mosquito

Aedes aegypti. Insect Biochem. Mol. Biol. **67**, 59-73. doi:10.1016/j.ibmb.2015.06.006

Piermarini, P. M., Akuma, D. C., Crow, J. C., Jamil, T. L., Kerkhoff, W. G., Viel, K. C. M. F. and Gillen, C. M. (2017). Differential expression of putative sodium-dependent cation-chloride cotransporters in *Aedes aegypti. Comp. Biochem. Physiol. A Physiol.* **214**, 40-49. doi:10.1016/j.cbpa.2017.09.007

Plant, L. D. and Goldstein, A. N. (2015). Two-pore domain potassium channels. In *Handbook of Ion Channels* (ed. J. Zhang and M. C. Trudeau), pp. 261-274. Boca Raton: CRC Press, Taylor & Francis.

Pullikuth, A. K., Aimanova, K., Kang'ethe, W., Sanders, H. R. and Gill, S. S. (2006). Molecular characterization of sodium/proton exchanger 3 (NHE3) from the yellow fever vector, *Aedes aegypti. J. Exp. Biol.* **209**, 3529-3544. doi:10.1242/jeb.02419

Riegel, J. A., Farndale, R. W. and Maddrell, S. (1999). Fluid secretion by isolated Malpighian tubules of *Drosophila melanogaster* Meig.: effects of organic anions, quinacrine and a diuretic factor found in the secreted fluid. *J. Exp. Biol.* **202**, 2339-2348.

Robertson, L., Chasiotis, H., Galperin, V. and Donini, A. (2014a). Allatostatin A-like immunoreactivity in the nervous system and gut of the larval midge *Chironomus riparius*: modulation of hindgut motility, rectal K^{+} transport and implications for exposure to salinity. *J. Exp. Biol.* **217**, 3815-3822. doi:10.1242/jeb.108985

Robertson, L., Donini, A. and Lange, A. B. (2014b). K^{+} absorption by locust gut and inhibition of ileal K^{+} and water transport by FGLamide allatostatins. *J. Exp. Biol.* **217**, 3377-3385. doi:10.1242/jeb.101774

Robinson, R. A. and Stokes, R. M. (1968). *Electrolyte Solutions*. London: Butterworths.

Roe, A. D., Demidovich, M. and Dedes, J. (2018). Origins and history of laboratory insect stocks in a multispecies insect production facility, with the proposal of standardized nomenclature and designation of formal standard names. *J. Insect. Sci.* **18**, 474-479. doi:10.1093/jisesa/iey037

Ruiz-Sanchez, E., O'Donnell, M. J. and Donini, A. (2015). Secretion of Na(+), K(+) and fluid by the Malpighian (renal) tubule of the larval cabbage looper *Trichoplusia ni* (Lepidoptera: Noctuidae). *J. Insect Physiol.* **82**, 92-98. doi:10.1016/j.jinsphys.2015.09.007

Ryerse, J. S. (1979). Developmental changes in Malpighian tubule cell structure. *Tissue Cell* **11**, 533-551. doi:10.1016/0040-8166(79)90061-2

Sajadi, F., Curcuruto, C., Al Dhaheri, A. and Paluzzi, J.-P. V. (2018). Anti-diuretic action of a CAPA neuropeptide against a subset of diuretic hormones in the disease vector *Aedes aegypti. J. Exp. Biol.* **221**, jeb177089. doi:10.1242/jeb.177089

Schönherr, R., Löber, K. and Heinemann, S. H. (2000). Inhibition of human ether à go-go potassium channels by Ca(2+)/calmodulin. *EMBO J.* **19**, 3263-3271. doi:10.1093/emboj/19.13.3263

Schulte, K., Kunter, U. and Moeller, M. J. (2015). The evolution of blood pressure and the rise of mankind. *Nephrol. Dialysis Transplant.* **30**, 713-723. doi:10.1093/ndt/gfu275

Shi, W. M., Wymore, R. S., Wang, H.-S., Pan, Z. M., Cohen, I. S., McKinnon, D. and Dixon, J. E. (1997). Identification of two nervous system-specific members of the erg potassium channel gene family. *J. Neurosci.* **17**, 9423-9432. doi:10.1523/JNEUROSCI.17-24-09423.1997

Siroky, B. J., Kleene, N. K., Kleene, S. J., Varnell, C. D., , Jr, Comer, R. G., Liu, J., Lu, L., Pachciarz, N. W., Bissler, J. J. and Dixon, B. P. (2017). Primary cilia regulate the osmotic stress response of renal epithelial cells through TRPM3. *Am. J. Physiol. Renal Physiol.* **312**, F791-F805. doi:10.1152/ajprenal.00465.2015

Skaer, N. J. V., Nässel, D. R., Maddrell, S. H. P. and Tublitz, N. J. (2002). Neurochemical fine tuning of a peripheral tissue: peptidergic and aminergic regulation of fluid secretion by Malpighian tubules in the tobacco hawkmoth *M. sexta. J. Exp. Biol.* **205**, 1869-1880.

Skerrett, I. M. and Williams, J. B. (2016). A structural and functional comparison of gap junction channels composed of connexins and innexins. *Dev. Neurobiol.* **77**, 522-547. doi:10.1002/dneu.22447

Stanley, D. and Kim, Y. (2019). Insect prostaglandins and other eicosanoids: From molecular to physiological actions. In *Advances in Insect Physiology*, Vol. **56** (ed. R. Jurenka), pp. 283-343. London, UK: Elsevier, Academic Press.

Vanderveken, M. and O'Donnell, M. J. (2014). Effects of diuretic hormone 31, drosokinin, and allatostatin a on transepithelial k +transport and contraction frequency in the midgut and hindgut of larval *Drosophila melanogaster. Arch. Insect Biochem. Physiol.* **85**, 76-93. doi:10.1002/arch.21144

Veenstra, J. A., Agricola, H.-J. and Sellami, A. (2008). Regulatory peptides in fruit fly midgut. *Cell Tissue Res.* **334**, 499-516. doi:10.1007/s00441-008-0708-3

Wang, C.-Y., Jenkitkasemwong, S., Duarte, S., Sparkman, B. K., Shawki, A., Mackenzie, B. and Knutson, M. D. (2012). ZIP8 is an iron and zinc transporter whose cell-surface expression is up-regulated by cellular iron loading. *J. Biol. Chem.* **287**, 34032-34043. doi:10.1074/jbc.M112.367284

Weihrauch, D., Donini, A. and O'Donnell, M. J. (2012). Ammonia transport by terrestrial and aquatic insects. *J. Insect Physiol.* **58**, 473-487. doi:10.1016/j.jinsphys.2011.11.005

Wigglesworth, V. B. (1961). *The Principles of Insect Physiology*, 5th edn, Vol. 279, pp. 367-373. Methuen & Co.

Wu, Y., Baum, M., Huang, C.-L. and Rodan, A. R. (2015). Two inwardly rectifying potassium channels, Irk1 and Irk2, play redundant roles in *Drosophila* renal tubule function. *Am. J. Physiol. Regul. Integr. Comp. Physiol.* **309**, R747-R756. doi:10.1152/ajpregu.00148.2015

Wulff, J. P., Sierra, I., Sterkel, M., Holtof, M., Van Wielendaele, P., Francini, F., Broeck, J. V. and Ons, S. (2017). Orcokinin neuropeptides regulate ecdysis in the hemimetabolous insect *Rhodnius prolixus. Insect Biochem. Mol. Biol.* **81**, 91-102. doi:10.1016/j.ibmb.2017.01.003

Xiao, G., Wan, Z., Fan, Q., Tang, X. and Zhou, B. (2014). The metal transporter ZIP13 supplies iron into the secretory pathway in *Drosophila melanogaster. eLife* **3**, 159-221. doi:10.7554/eLife.03191

Xu, J., Wan, Z. and Zhou, B. (2019). Drosophila ZIP13 is posttranslationally regulated by iron-mediated stabilization. *Biochim. Biophys. Act. Mol. Cell Res.* **1866**, 1487-1497. doi:10.1016/j.bbamcr.2019.06.009

Yamanaka, N., Roller, L., Žitňan, D., Satake, H., Mizoguchi, A., Kataoka, H. and Tanaka, Y. (2010). Bombyx orcokinins are brain-gut peptides involved in the neuronal regulation of ecdysteroidogenesis. *J. Comp. Neurol.* **519**, 238-246. doi:10.1002/cne.22517

Yang, H. and Cui, J. (2015). BK channels. In *Handbook of Ion Channels* (ed. J. Zhang and M. C. Trudeau), pp. 227-240. Boca Raton: CRC Press, Taylor & Francis.

Young, M. D., Wakefield, M. J., Smyth, G. K. and Oshlack, A. (2010). Gene ontology analysis for RNA-seq: accounting for selection bias. *Genome Biol.* **11**, R14.

Yuan, A., Santi, C. M., Wei, A., Wang, Z.-W., Pollak, K., Nonet, M., Kaczmarek, L., Crowder, C. M. and Salkoff, L. (2003). The sodium-activated potassium channel is encoded by a member of the Slo gene family. *Neuron* **37**, 765-773. doi:10.1016/S0896-6273(03)00096-5

Zandawala, M. (2012). Calcitonin-like diuretic hormones in insects. *Insect Biochem. Mol. Biol.* **42**, 816-825. doi:10.1016/j.ibmb.2012.06.006

Zhu, M. X., Evans, M. D., Ma, J., Parrington, J. and Galione, A. (2010). Two-pore channels for integrative Ca^{2+} signaling. *Communic. Integr. Biol.* **3**, 12-17. doi:10.4161/cib.3.1.9793